Nb-Ti joints

Glyn Kirby

Overview

- Quick look at Fusillo and its sub-scale coil
- A look at Nb-Ti joint designs
- A look at winding CCT coil

Base line design V17 cold

- Field at Center point : 3.0000 T
- Current : **289.498** A
- Central inner coil radius R=128mm , 5 mm tapered slop over coil length. A= skew, B=Normal
- Combined functions: Dipole A1 =-0.003 mm B2=212.64 mm, Quad A2= -0.05 mm B2 -3.05 mm, Sextupole A3= 0.01 mm B3=0.08 , Octupole B4=0.01 mm,
- Peak field inner/outer coils : 3.562 , 3.447 T
- Load line Fraction inner/outer coils at 4.5K : 60.768% , 59.528%
- Integral on 1m rad axis 90 deg over 3.5m Tm : By -2.878, Bx -6.24 e-05, Bz 8.145 e-3
- Dipole Field variation over central area 100mm dia ~ 2 gauss :
- Inductance : 9.296H
- Energy : 388.28 kJ
- 7 strand *insulated* rope , 10 ropes in channel. Log stacking lay out 70 strands in total.
- Joints : 70 + 1 =71 at lead end
- Strand and cable for the demo coil : ~13.1 km strand , ~1.87 km rope.
- 1m rad of curvature ***cold!!.***
- 90 deg end to end angle at the outside of the magnet
- Former : Spar ~ 5 mm, min wall 0.5 mm, at magnet ends it increases.
- Channel size log stacking : width = 5.88 mm x Depth = 17.1 mm WARM

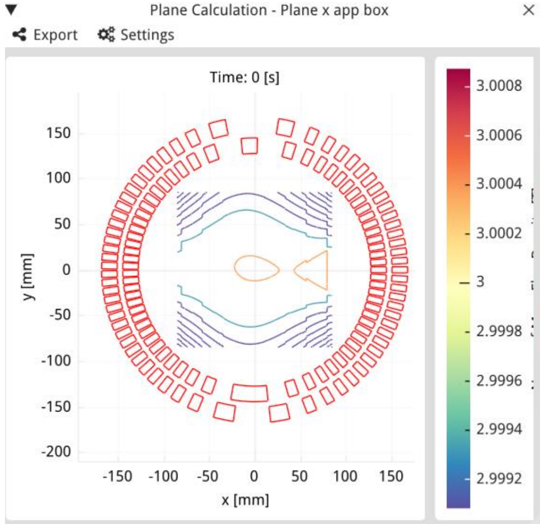

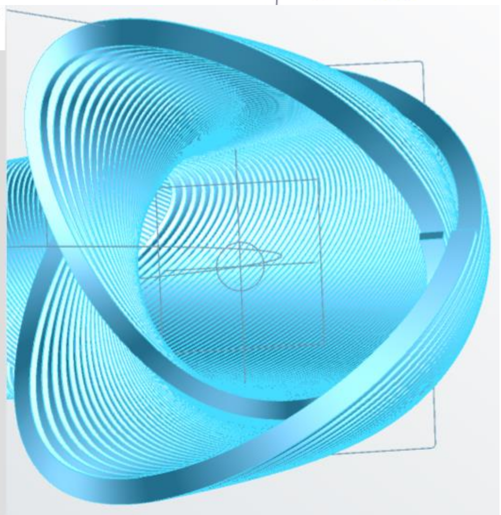

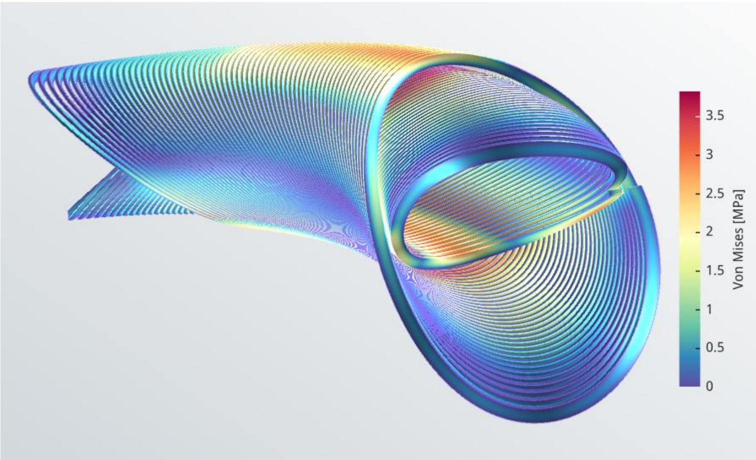

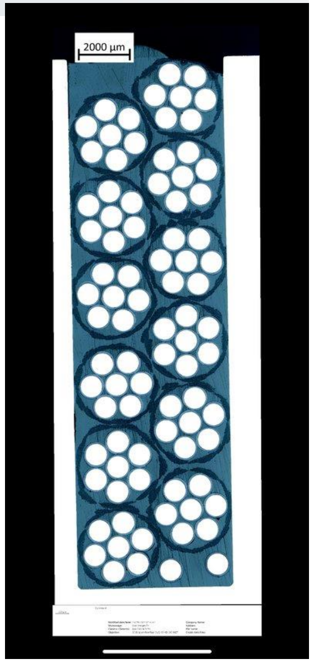

Sub Scale design

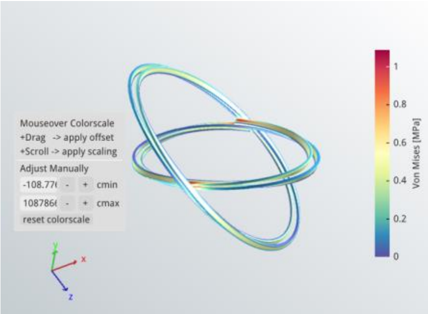

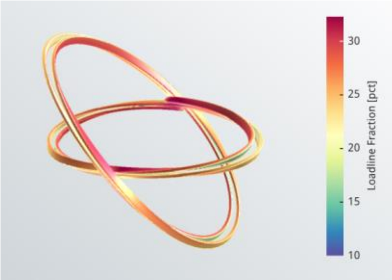

1.08 MPa @ **289.097** A, 32% ss 3.168K margin

Scaling from SS% 60/32= 540A

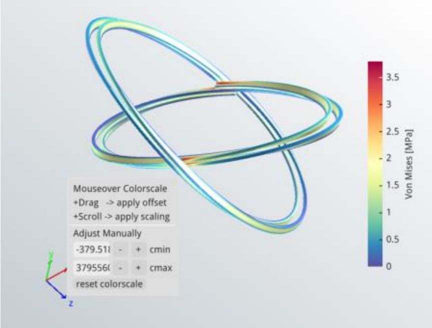

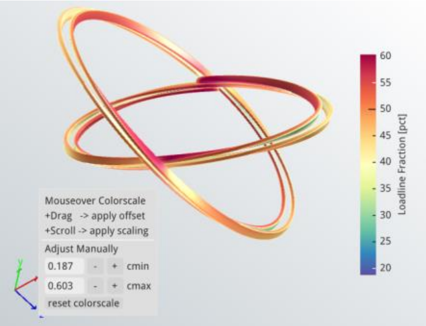

3.8 MPa @ **540** A, 60.3% ss 1.98K margin
2.09T

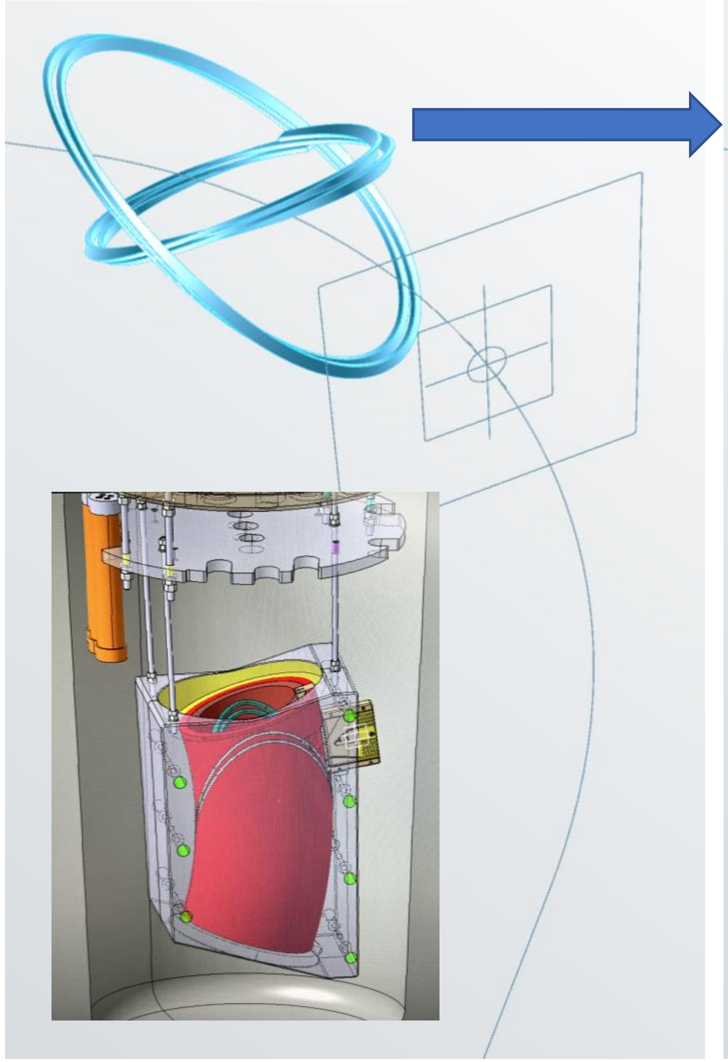

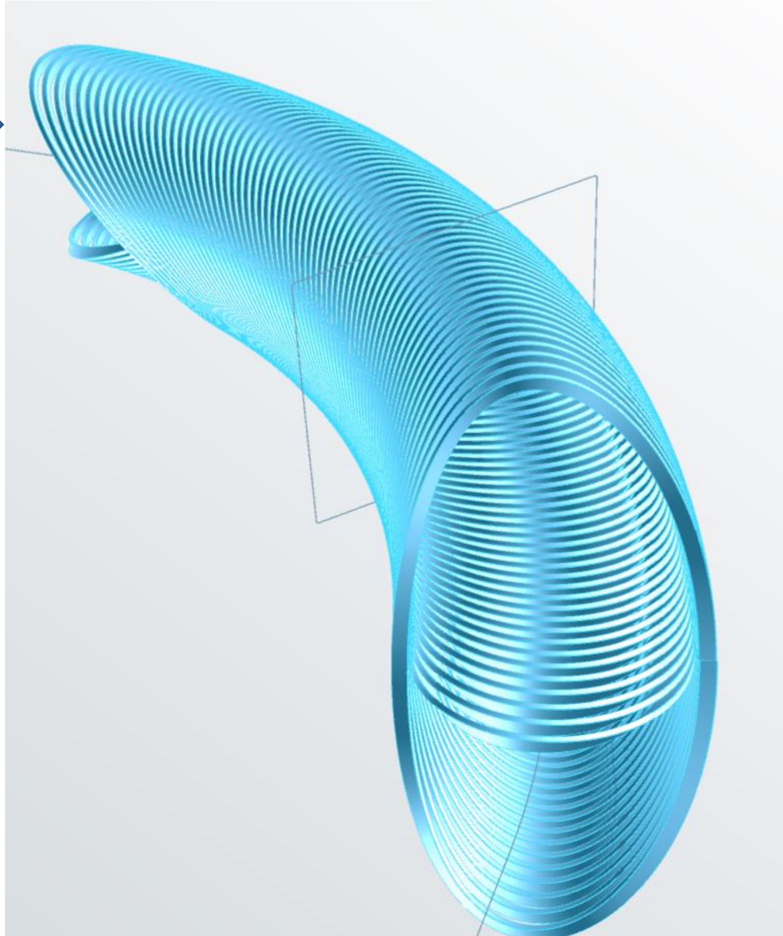

3.8 MPa @ **289**A, 60.7 %SS
1.97 K margin

Sub-scale used the last few turns, for the full then runs at higher current to match stress and short sample

Sub Scale load line

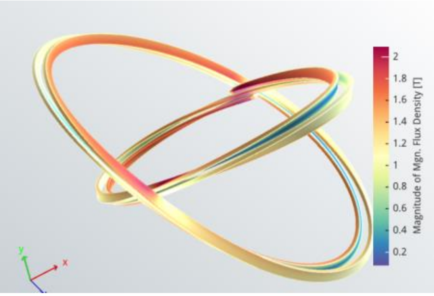

Nom Current 540A
Inductance 39.779 mH

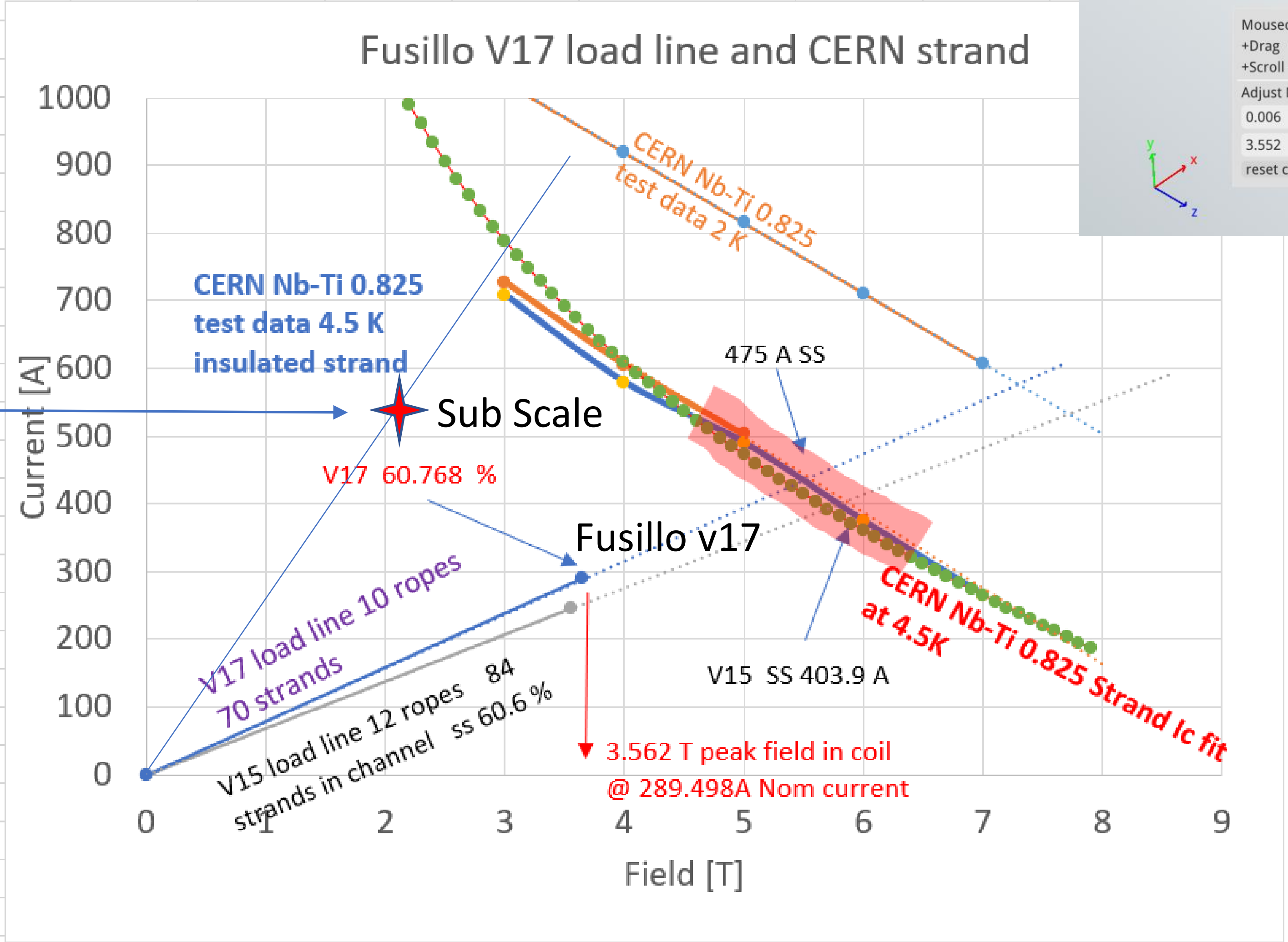

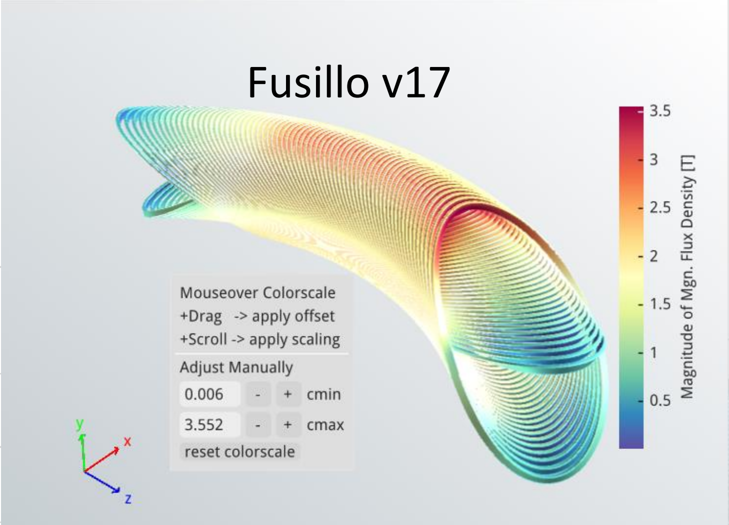

Fusillo

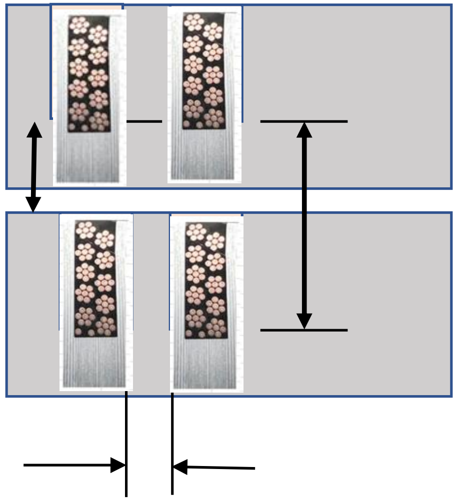

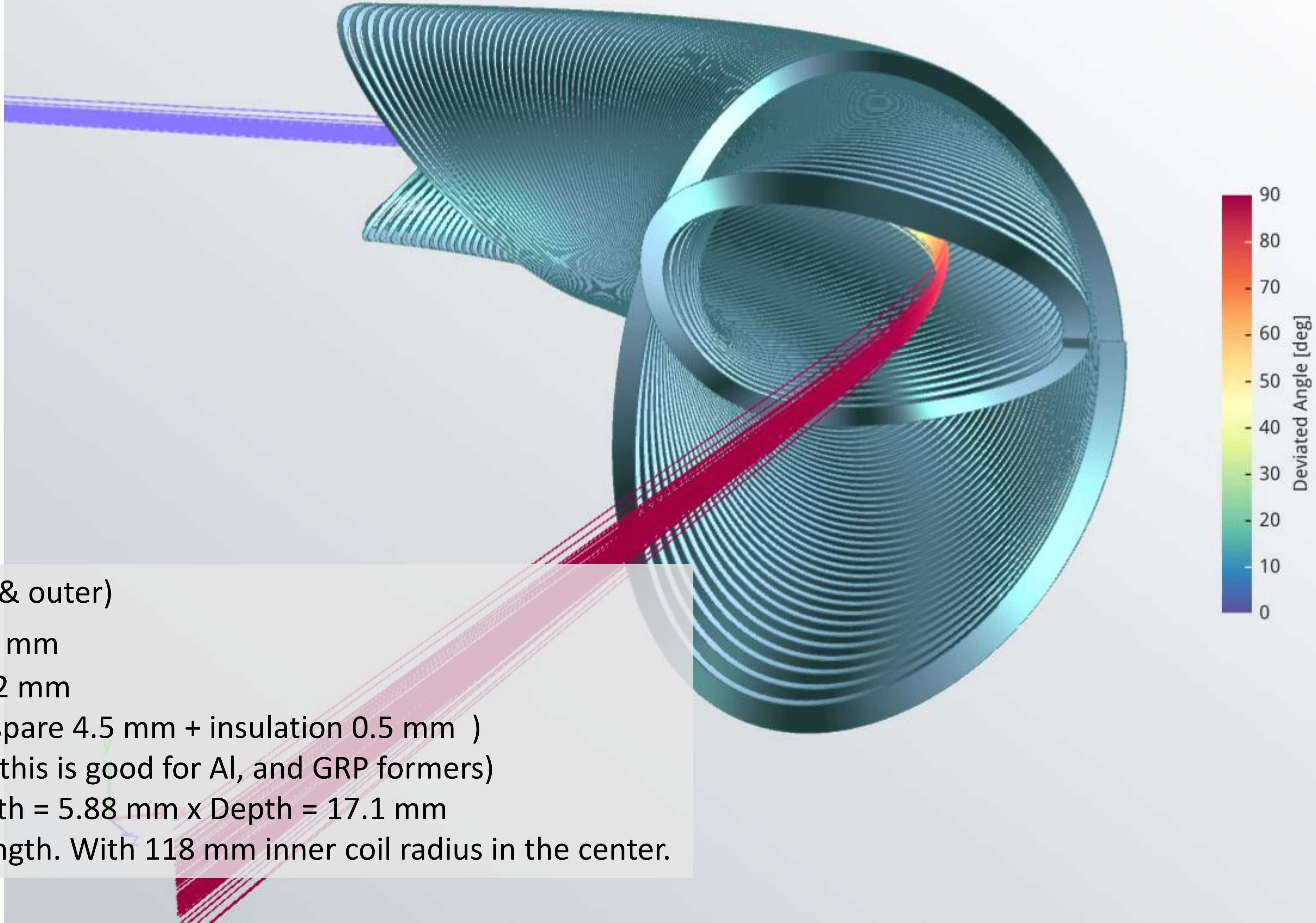

66 turns in the formers (inner & outer)

Inner *coil* center radius = 128 mm

Distance between layers = 23.2 mm

Spacer between coil = 5 mm (spare 4.5 mm + insulation 0.5 mm)

Min wall thickness = 0.5 mm (this is good for Al, and GRP formers)

Channel size log stacking : width = 5.88 mm x Depth = 17.1 mm

Taper = 10mm over the coil length. With 118 mm inner coil radius in the center.

Joints

We talk about prying hands and shaking hand joints

Joint layout types

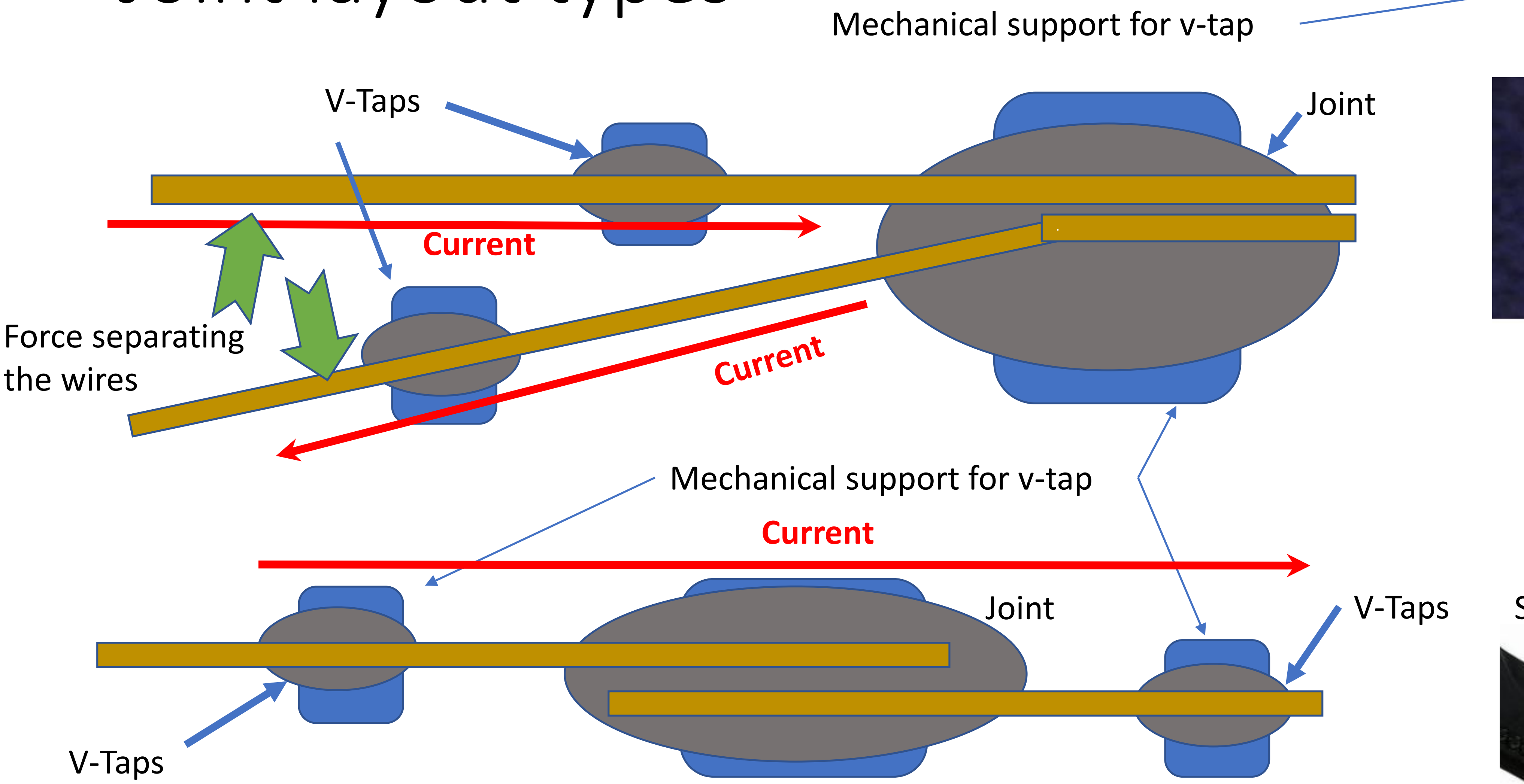

Prying hands joint

Shaking hands joint

Prying hands current distribution

[9727200.pdf (kek.jp)]

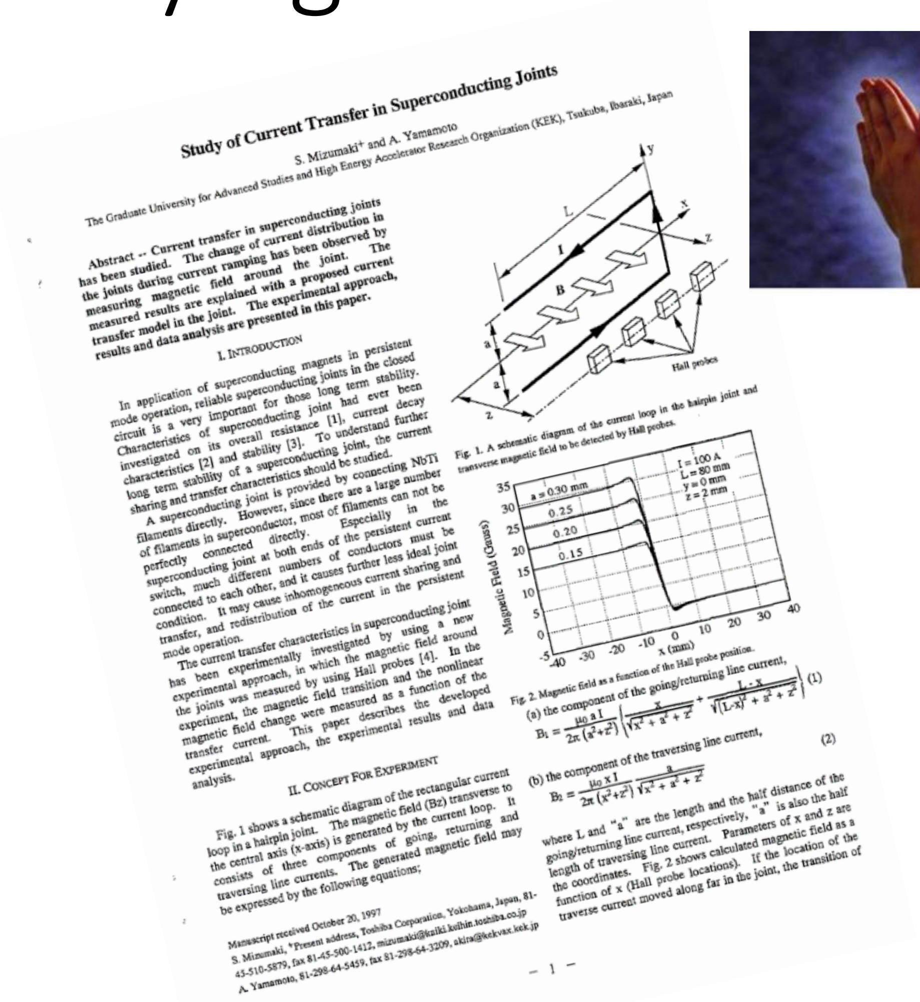

Study of Current Transfer in Superconducting Joints

S. Mizumaki* and A. Yamamoto

The Graduate University for Advanced Studies and High Energy Accelerator Research Organization (KEK), Tsukuba, Ibaraki, Japan

Abstract -- Current transfer in superconducting joints has been studied. The change of current distribution in the joints during current ramping has been observed by measuring magnetic field around the joint. The measured results are explained with a proposed current transfer model in the joint. The experimental approach, results and data analysis are presented in this paper.

I. INTRODUCTION

In application of superconducting magnets in persistent mode operation, reliable superconducting joints in the closed circuit is a very important for those long term stability. Characteristics of superconducting joint had ever been investigated on its overall resistance [1], current decay characteristics [2] and stability [3]. To understand further long term stability of a superconducting joint, the current sharing and transfer characteristics should be studied.

A superconducting joint is provided by connecting NbTi filaments directly. However, since there are a large number of filaments in superconductor, most of filaments can not be perfectly connected directly. Especially in the superconducting joint at both ends of the persistent current switch, much different numbers of conductors must be connected to each other, and it causes further less ideal joint condition. It may cause inhomogeneous current sharing and transfer, and redistribution of the current in the persistent mode operation.

The current transfer characteristics in superconducting joint has been experimentally investigated by using a new experimental approach, in which the magnetic field around the joints was measured by using Hall probes [4]. In the experiment, the magnetic field transition and the nonlinear magnetic field change were measured as a function of the transfer current. This paper describes the developed experimental approach, the experimental results and data analysis.

II. CONCEPT FOR EXPERIMENT

Fig. 1 shows a schematic diagram of the rectangular current loop in a hairpin joint. The magnetic field (Bz) transverse to the central axis (x-axis) is generated by the current loop. It consists of three components of going, returning and traversing line currents. The generated magnetic field may be expressed by the following equations;

Fig. 1. A schematic diagram of the current loop in the hairpin joint and transverse magnetic field to be detected by Hall probes.

Fig. 2. Magnetic field as a function of the Hall probe position.

(a) the component of the going/returning line current,

$$B_1 = \frac{\mu_0 a I}{2\pi (a^2+z^2)} \left(\frac{x}{\sqrt{x^2+a^2+z^2}} + \frac{L-x}{\sqrt{(L-x)^2+a^2+z^2}} \right) \quad (1)$$

(b) the component of the traversing line current,

$$B_2 = \frac{\mu_0 x I}{2\pi (x^2+z^2)} \frac{a}{\sqrt{x^2+a^2+z^2}} \quad (2)$$

where L and "a" are the length and the half distance of the going/returning line current, respectively, "a" is also the half length of traversing line current. Parameters of x and z are the coordinates. Fig. 2 shows calculated magnetic field as a function of x (Hall probe locations). If the location of the traverse current moved along far in the joint, the transition of the

Manuscript received October 20, 1997

S. Mizumaki, *Present address, Toshiba Corporation, Yokohama, Japan, 81-45-510-5879, fax 81-45-500-1412, mizumaki@kaiki.keihin.toshiba.co.jp

A. Yamamoto, 81-298-64-5459, fax 81-298-64-3209, akira@kekvax.kek.jp

– 1 –

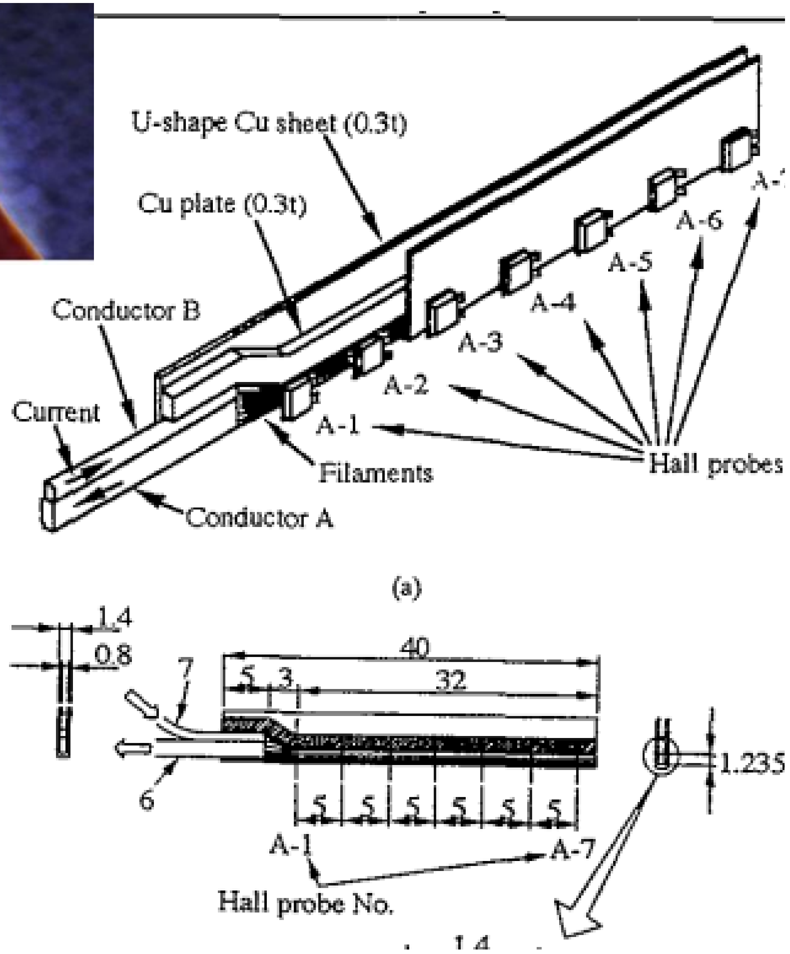

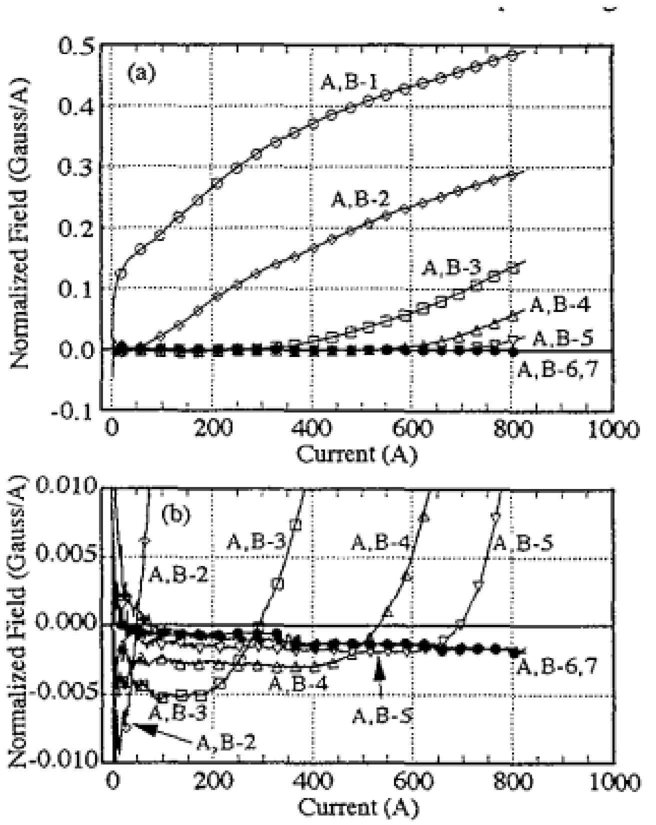

Fig. 6. (a) Normalized magnetic field as a function of the overall transfer current, (b) the expanded normalized magnetic field in the vertical scale.

It starts with Low Current crossing over to the other wire at the first opportunity. As the current increases the it moves further along the joint.

In this experiment hall probes measured the field generated by the current.

Shaking hands power distribution

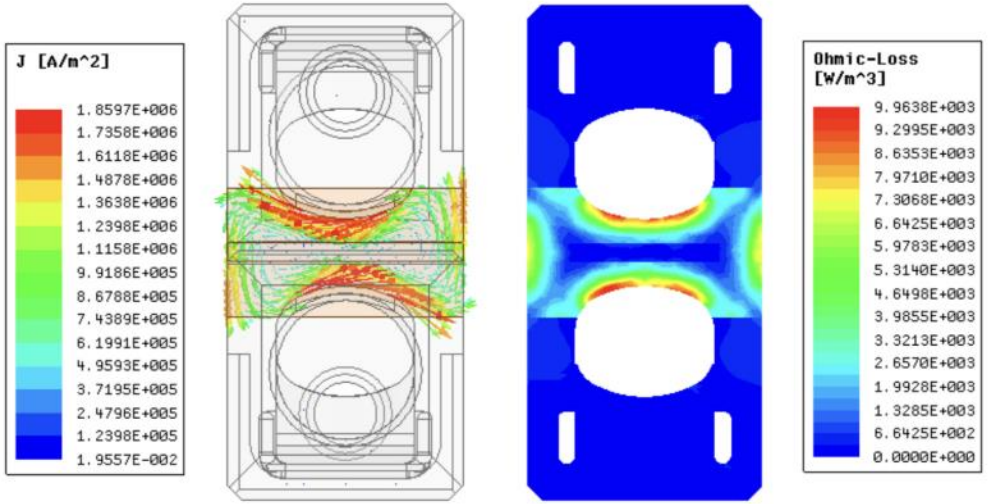

Fig. 75: Induced current (left) and ohmic loss distribution (right) in *X-Y* section view of PF6 DP joint for a 0.5 T/s field ramp along *z* axis.

77

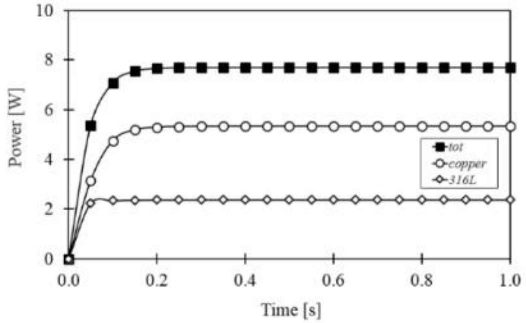

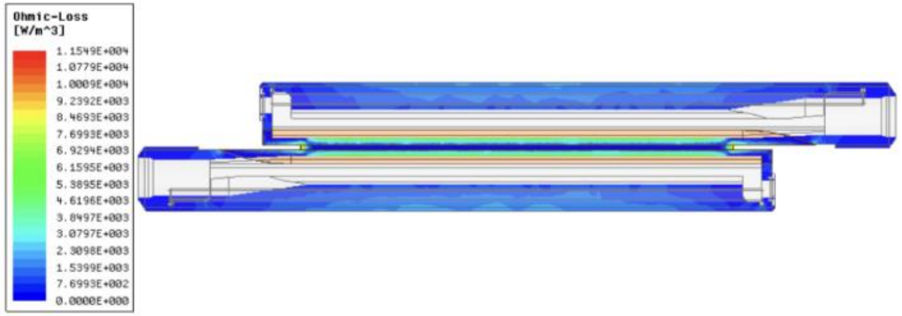

Fig. 73: Transient response (top) and ohmic loss distribution in *Y-Z* section view of PF6 DP joint (bottom) for a 0.5 T/s field ramp along *x* axis.

76

Joint testing

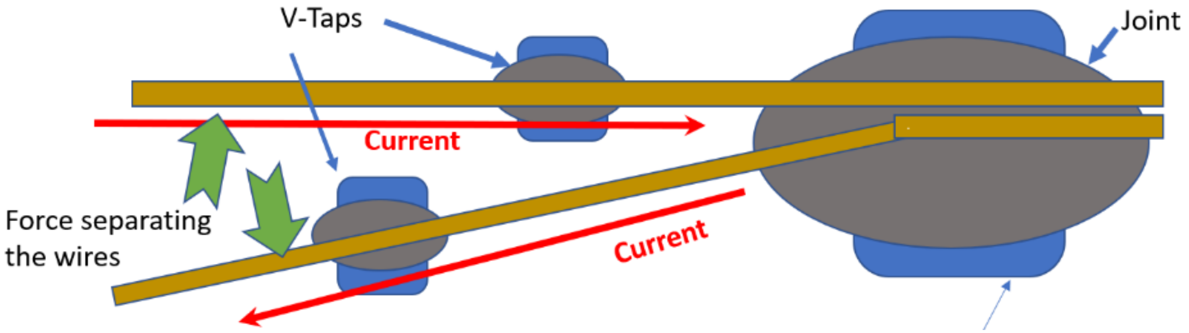

The voltage tap wires must not be in the same solder as the joint!
Also due to the common problem of dry joints the connections need a mechanical support on top of the soldered connection.

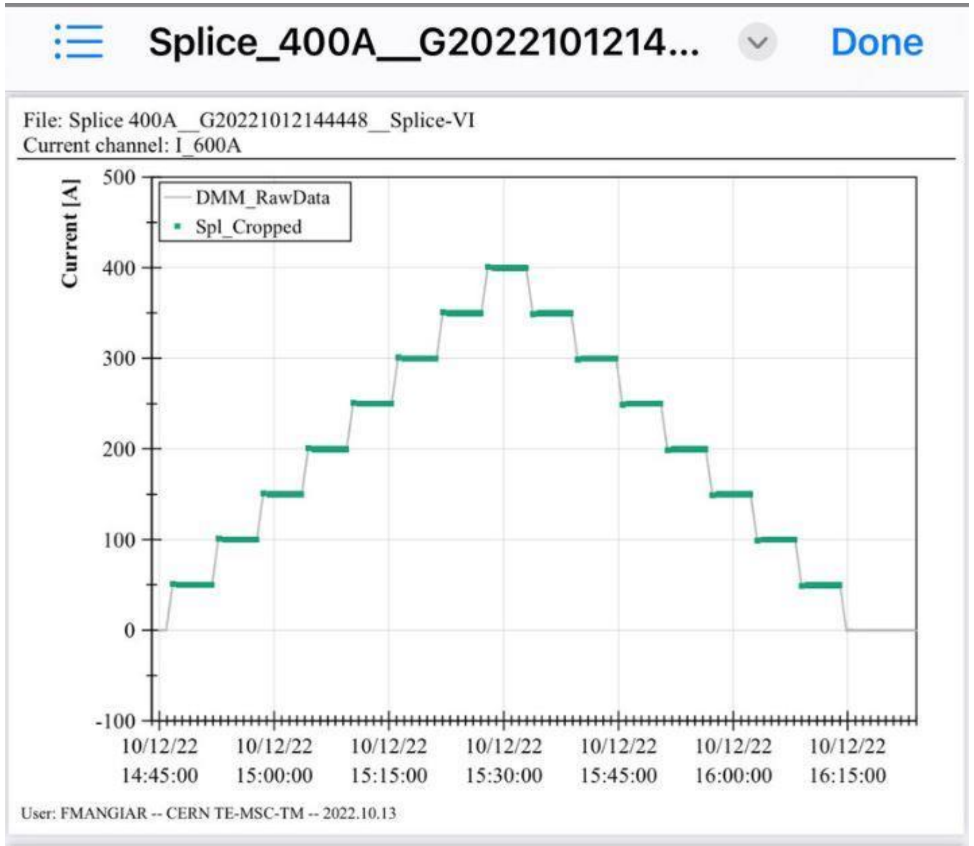

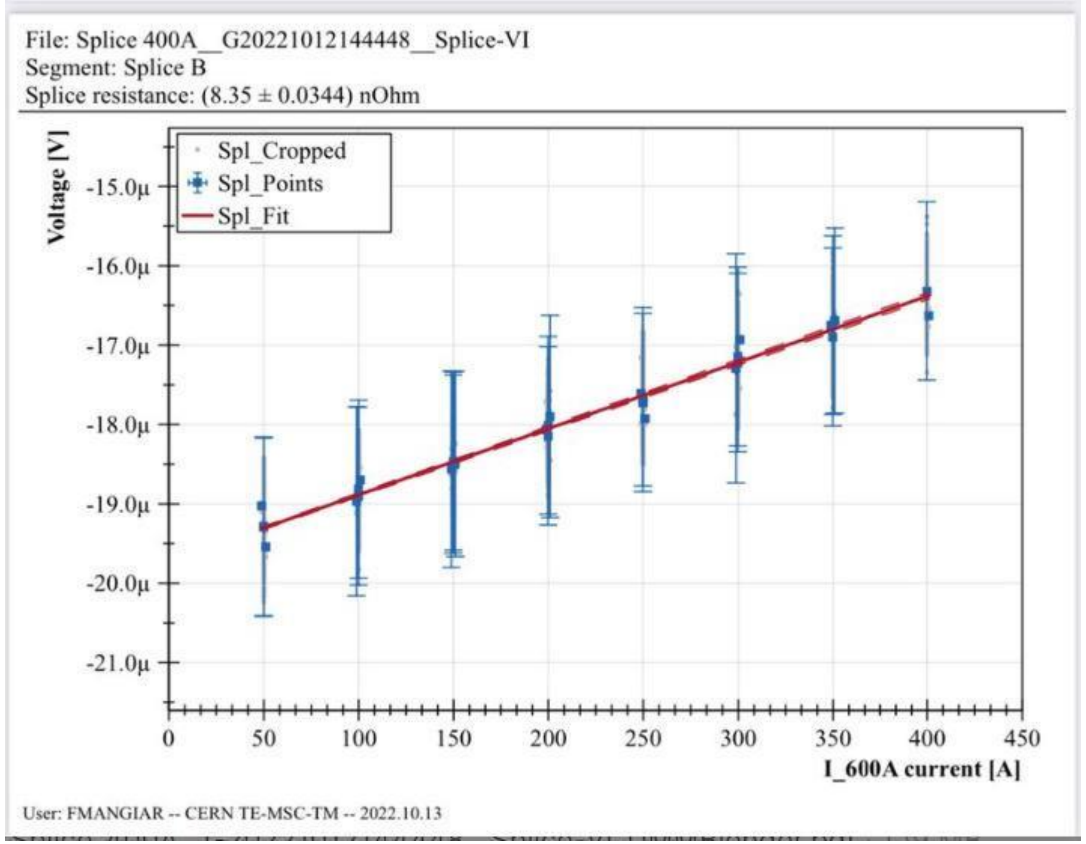

To measure the joint resistance, use a stare case current ladder. Up and down with plateaus

MCBRD joint design

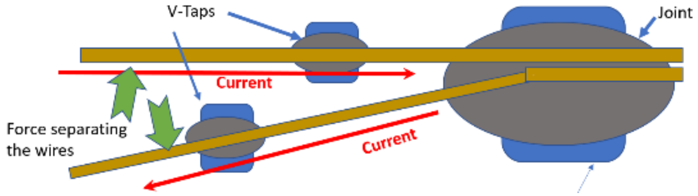

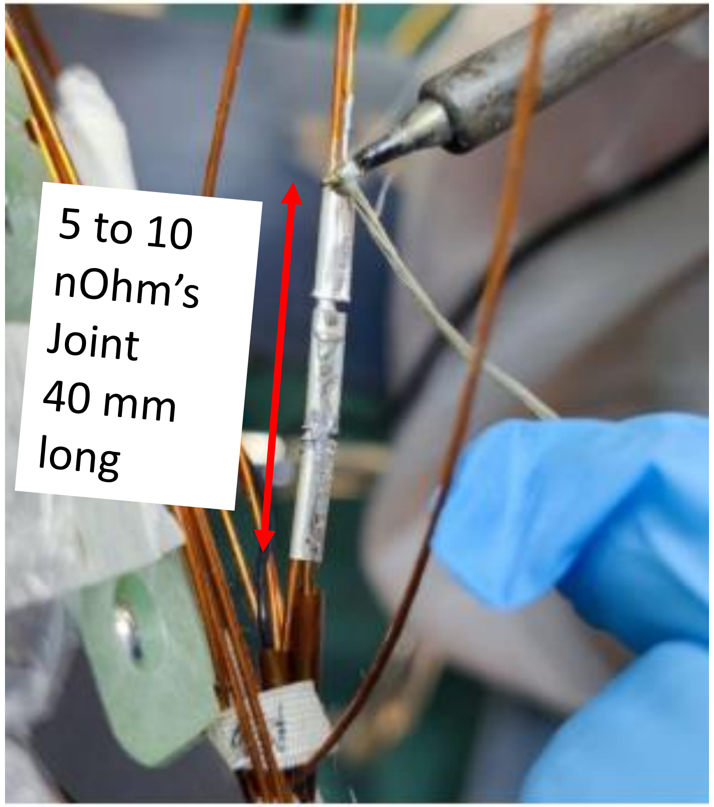

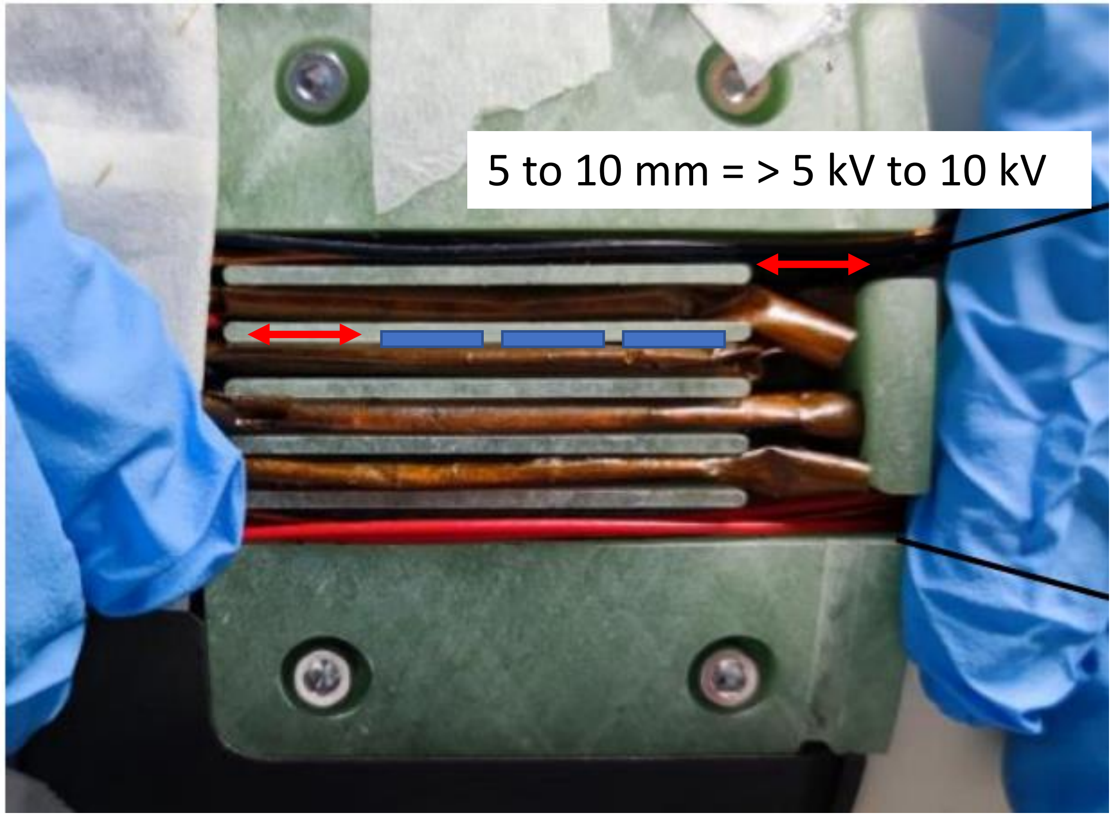

Insulation design at the joints is critical as it's the place where the cable insulation stops! The joint insulation should extend 5 to 10 mm past the end of the joint and where the cable insulation stope

CERN test results in liquid 4.5K

I would like to have 1 nOhm so they are still high at 4 to 8 nOhms but work in liquid

MCBRD Splice resistance with different design					
splice identification	Resistance nΩ	Tolerance +-	Average	std deviation	Remark
B	8.35	0.0344	7.64	1.30	standard ≈40mm
C	6.14	0.0379			
D	8.44	0.0314			
E	8.82	0.0349	8.01	0.80	length x2 ≈80mm
F	7.98	0.0354			
G	7.23	0.034			
H	3.45	0.0379	3.53	0.16	Cu removed (10% less)
I	3.71	0.0366			
J	3.43	0.0354			
K	3.1	0.0315	4.08	1.42	Helix pitch 12/13mm standard process and length ≈40mm
L	5.7	0.0399			
M	3.43	0.0321			
N	6.38	0.0339	5.93	0.57	Helix pitch 12/13mm standard process and length x2 ≈80mm
O	5.28	0.0341			
P	6.12	0.0309			

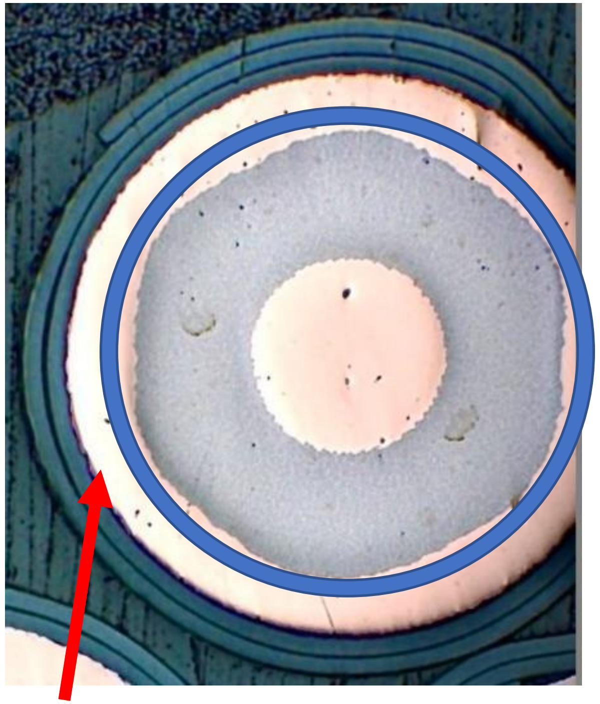

Removed copper outside of the blue line

Joint tests om 0.3mm dia wire f(joint length)

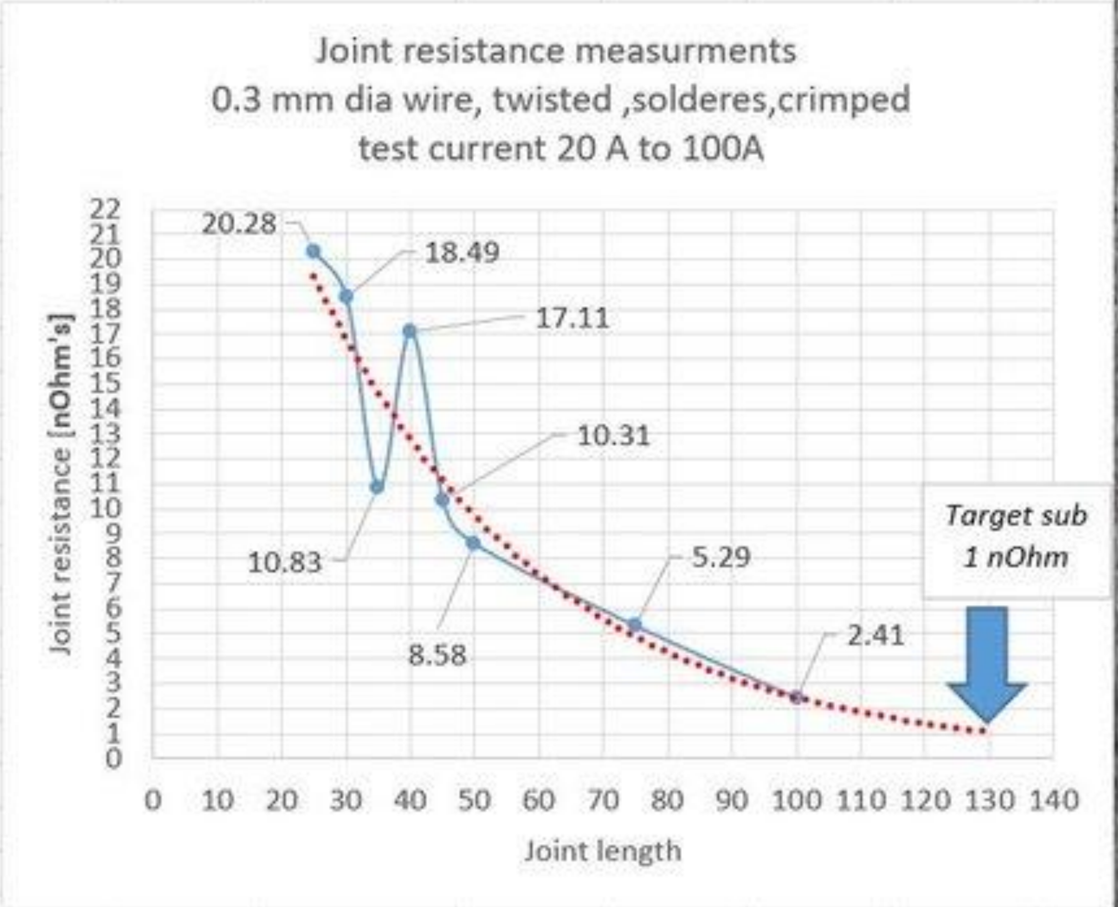

Very low resistance, Persistent joints

Composite Solder Production

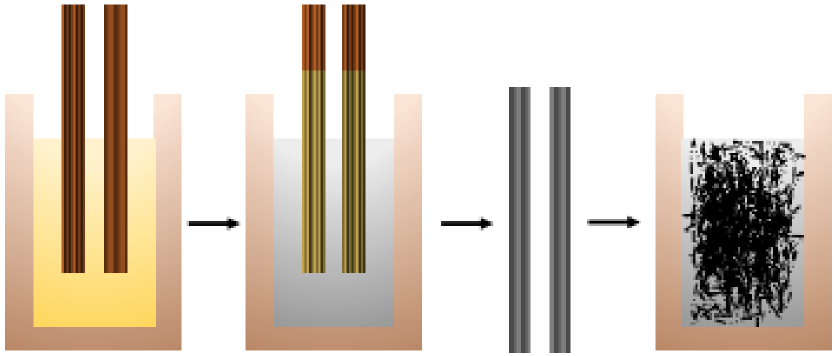

Composite $Bi_{15}In_{50}Sn_{35}$/NbTi solders are made from NbTi wire containing ~12,000 filaments each 3 µm in diameter. This wire is placed in liquid tin for 90 minutes at 370°C to replace the copper matrix with tin. The tin coated filaments are then placed in liquid $Bi_{15}In_{50}Sn_{35}$ solder at 250°C for 60 minutes to coat them in solder. The wire is then chopped and the pieces melted together and agitated to form the composite solder.

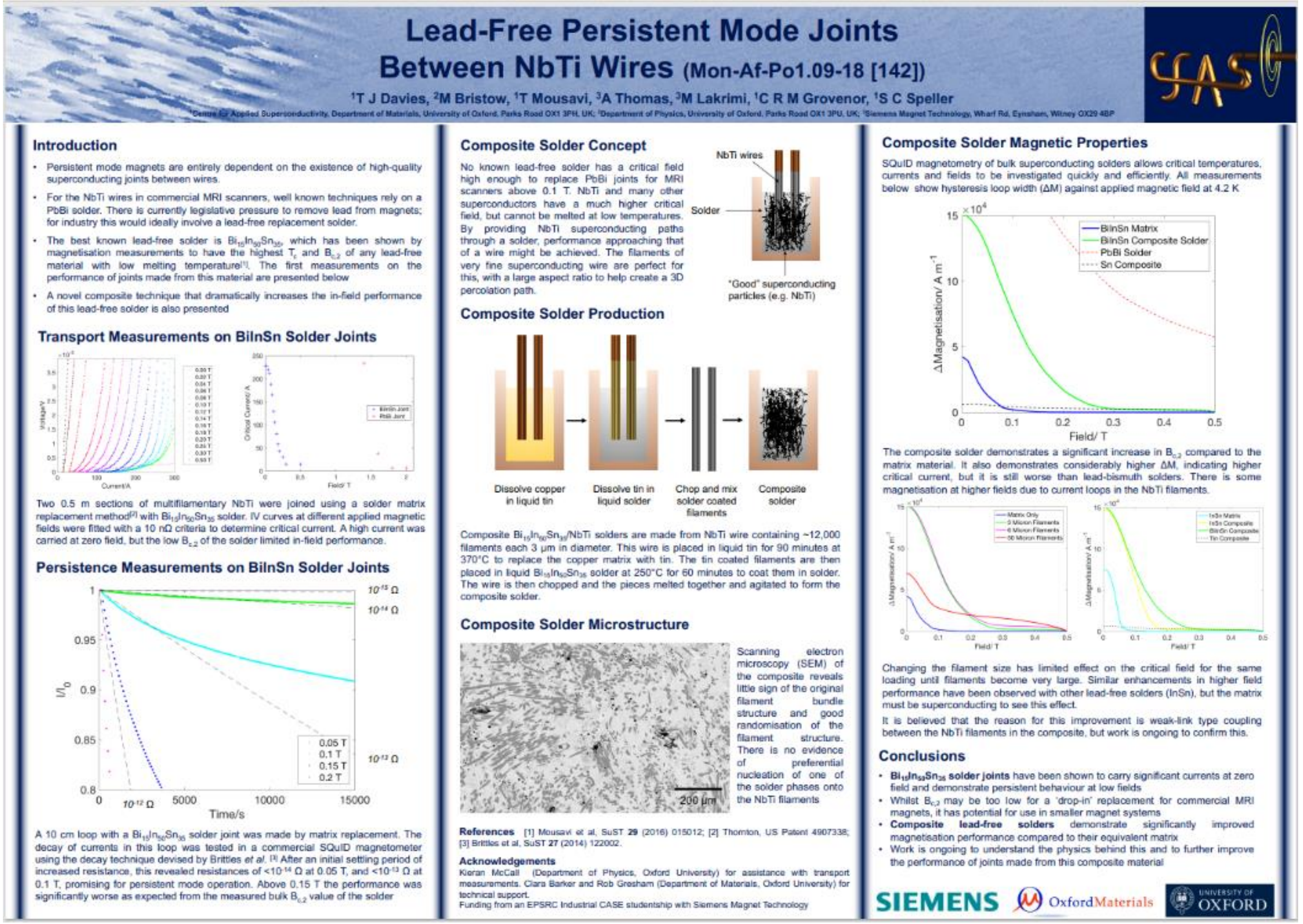

Pb42.5Bi55.5

[Niobium-titanium (Nb-Ti) superconducting joints for persistent-mode operation (nature.com)]

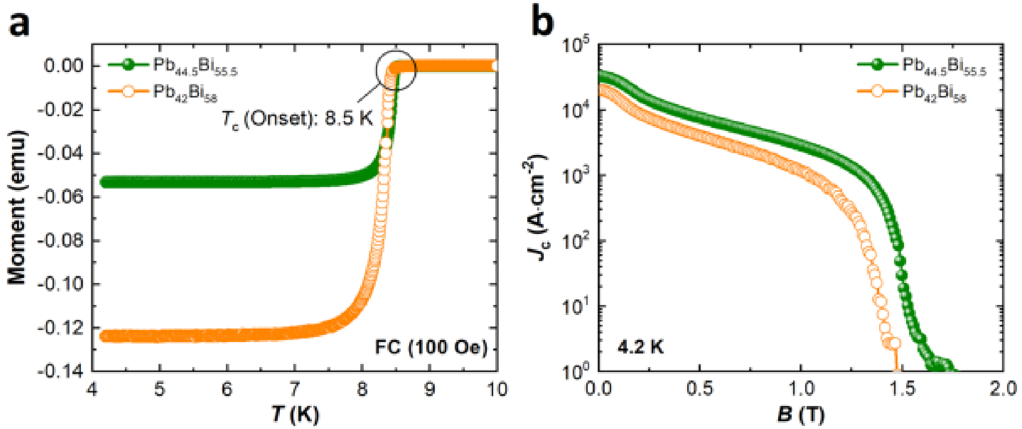

Figure 2. (**a**) Magnetic moment of the solders versus temperature under field cooling (FC) in self-field; (**b**) critical current density versus magnetic field characteristics measured using a physical property measurement system (PPMS).

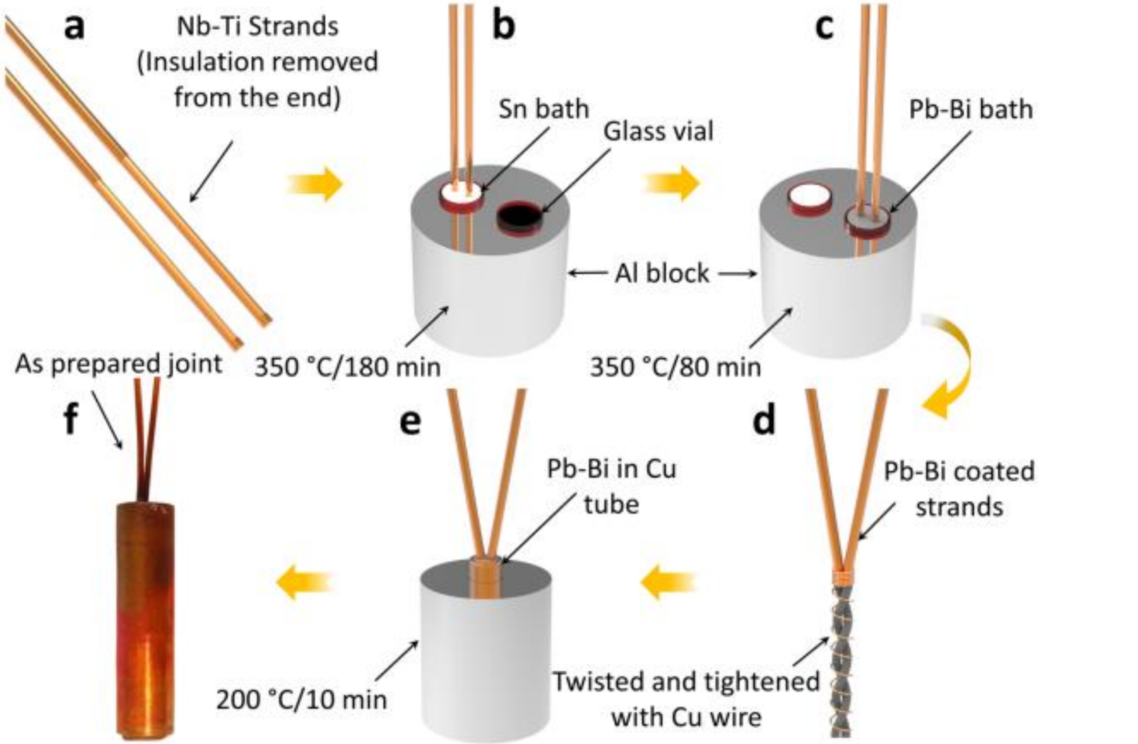

Figure 3. Joint fabrication process for multifilamentary Nb-Ti conductors using the solder matrix replacement method.

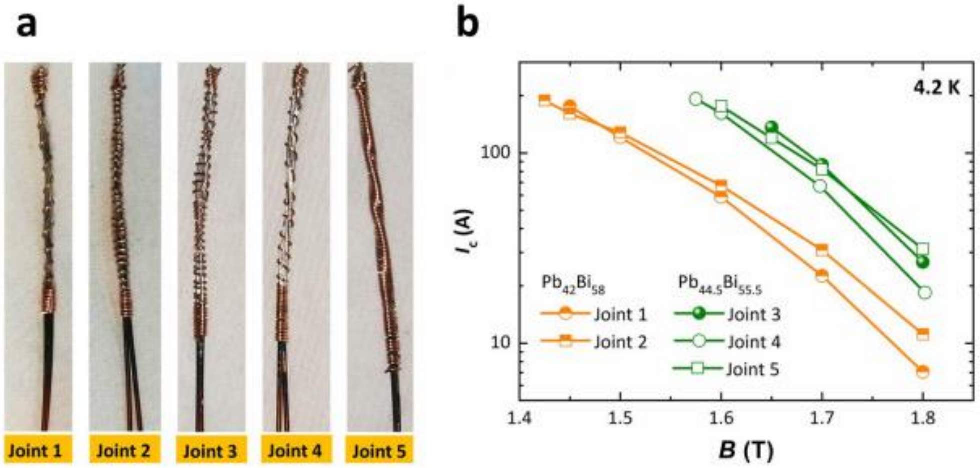

Figure 4. (**a**) Different types of Cu wire binding on joints 1 to 5, (**b**) critical current versus magnetic field characteristics of the joints.

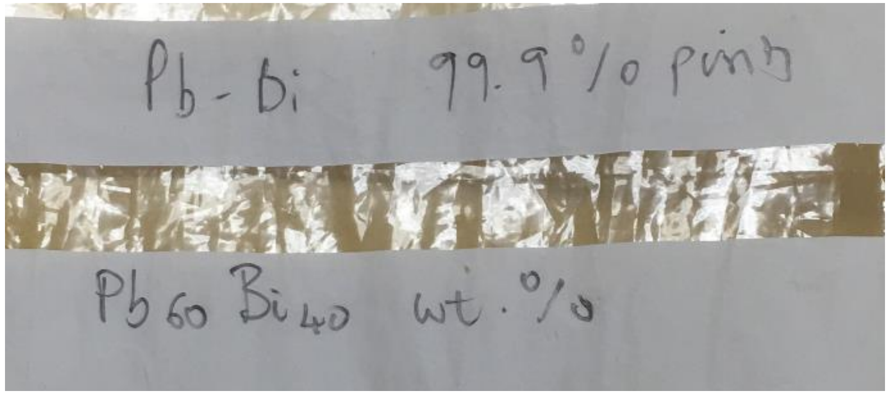

Superconducting Solder

Superconducting at 4K and < 1000 gauss

1000 gauss

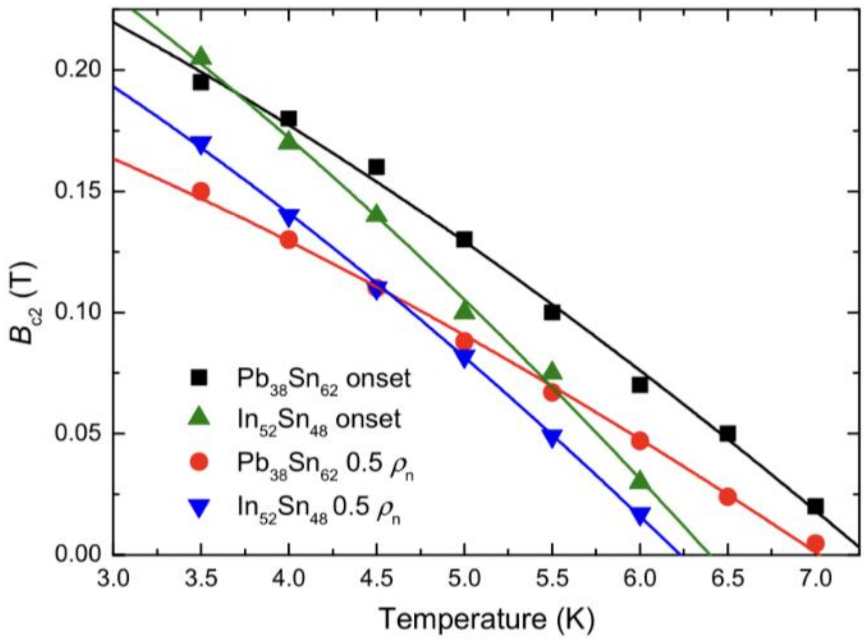

Figure 5. The normalised resistivity of $Pb_{38}Sn_{62}$ (upper) and $In_{52}Sn_{48}$ (middle) solders as a function of (increasing) applied magnetic fields at low temperatures. Lines are guide to the eye. Lower: upper critical field (B_{c2}) of $Pb_{38}Sn_{62}$ and $In_{52}Sn_{48}$ solders as a function of temperature. B_{c2} defined using two criteria: at the onset of transition (solid triangles and squares) and when the solder resistance equalled half of the normal state value (solid down triangles and circles). Curves are fitted using the W–H–H equation [75] and the derived parameters obtained are listed in table 6.

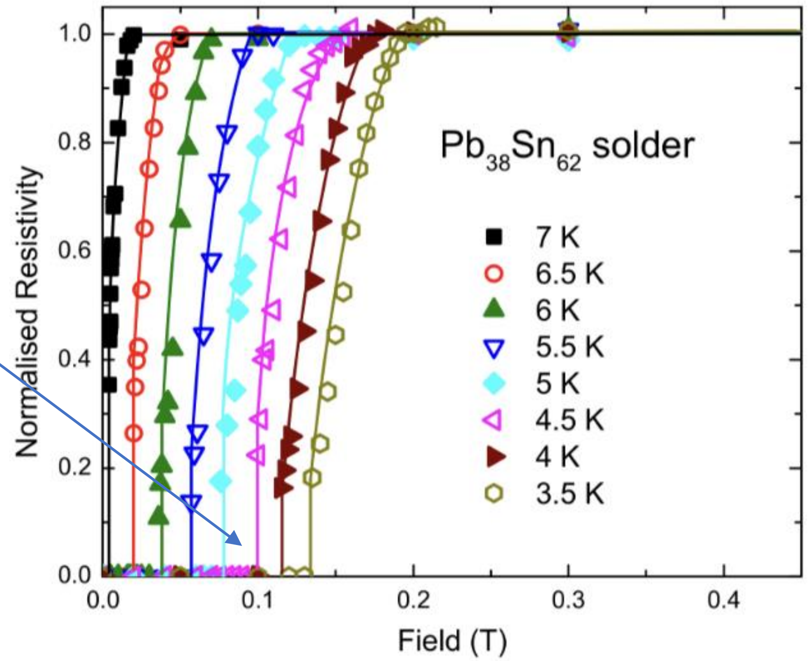

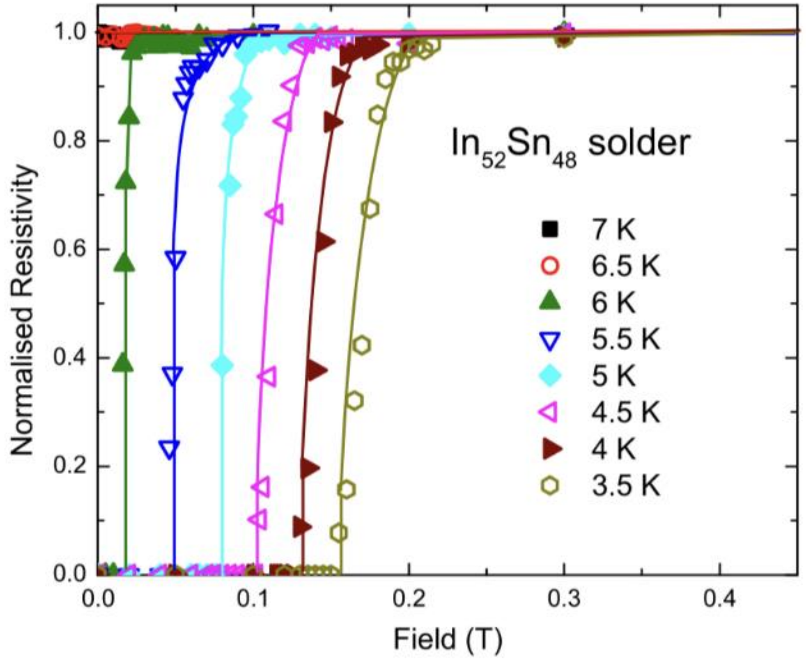

Bismuth joints 10e-14 Ohm’s

- Persistent joints
- Pros : low resistance just about superconductive, lends itself to persistent mode operation and conduction cooling.
- Cons: several processes available but are Complex, need to remove copper with Acid, overcome the oxide layer on the Nb-Ti tin bath, build joint in fume-cupboard , 350 C short time not to damage superconducting Nb-Ti material starts to be damaged at 400C =-10 %
- We could think to make a combination use the pots with bismuth and remove some copper ?

see link to Greg’s Phd on persistent joints

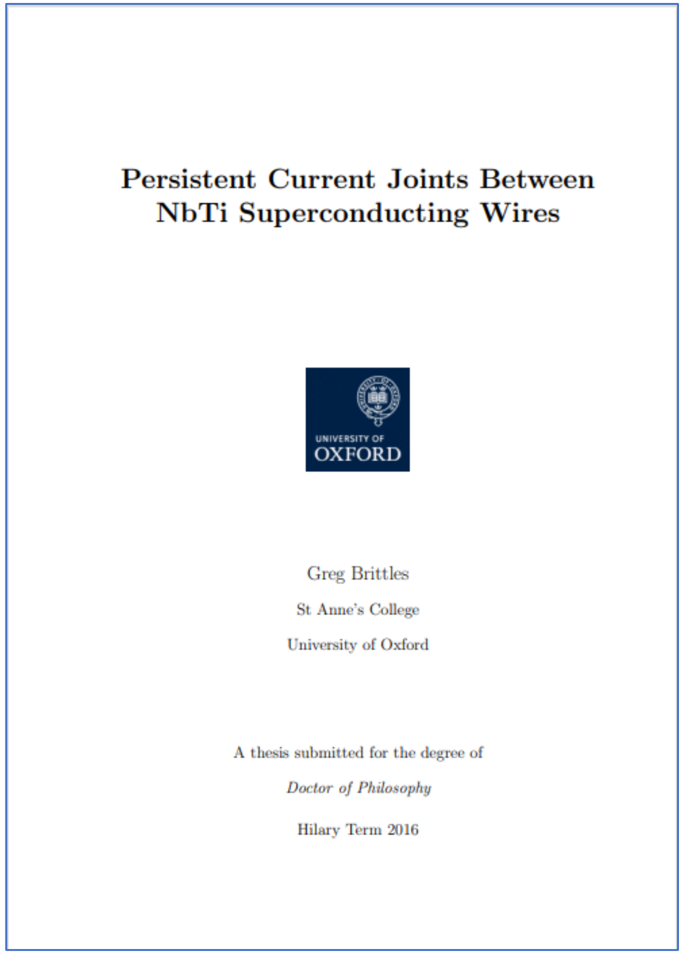
Persistent Current Joints Between NbTi Superconducting Wires

Greg Brittles

St Anne’s College

University of Oxford

A thesis submitted for the degree of

Doctor of Philosophy

Hilary Term 2016

A must read!

Greg

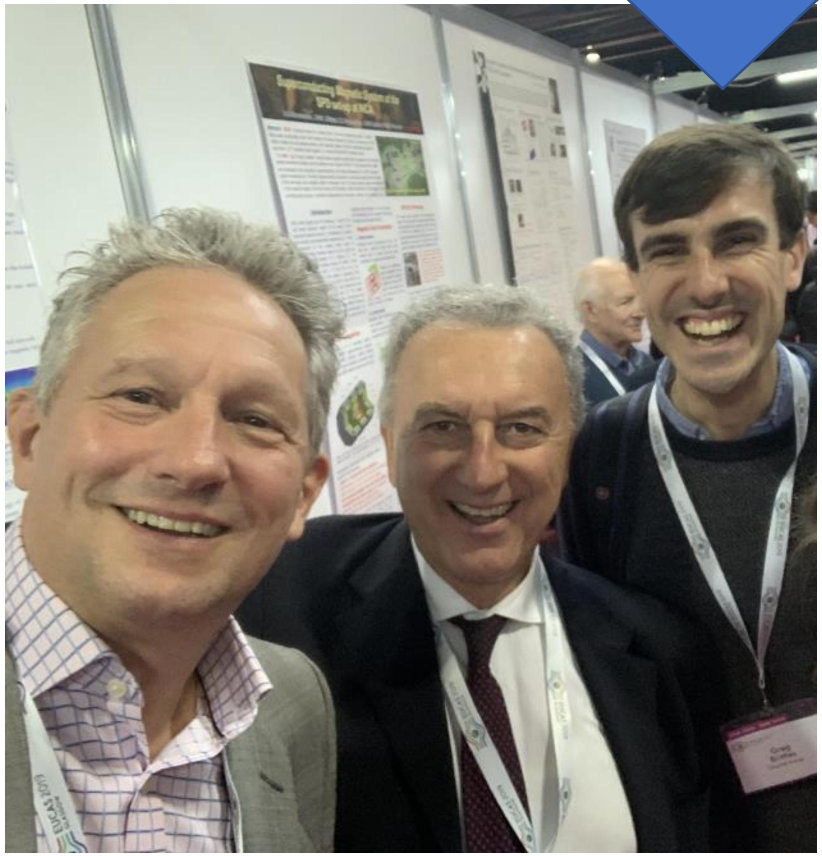

Greg's PhD covers all the types of persistent Join processes and chemistry.

[download file (ox.ac.uk)]

Persistent Current Joints Between NbTi Superconducting Wires

Greg Brittles

St Anne's College

University of Oxford

A thesis submitted for the degree of

Doctor of Philosophy

Hilary Term 2016

Joint pots

Joint pots offer low resistance are good for conduction cooling, they also provide magnetic field shielding with the 150 – 200 mm long twisted wire joint that is inside the pot !

Electrical insulation in this case is the gap in liquid helium

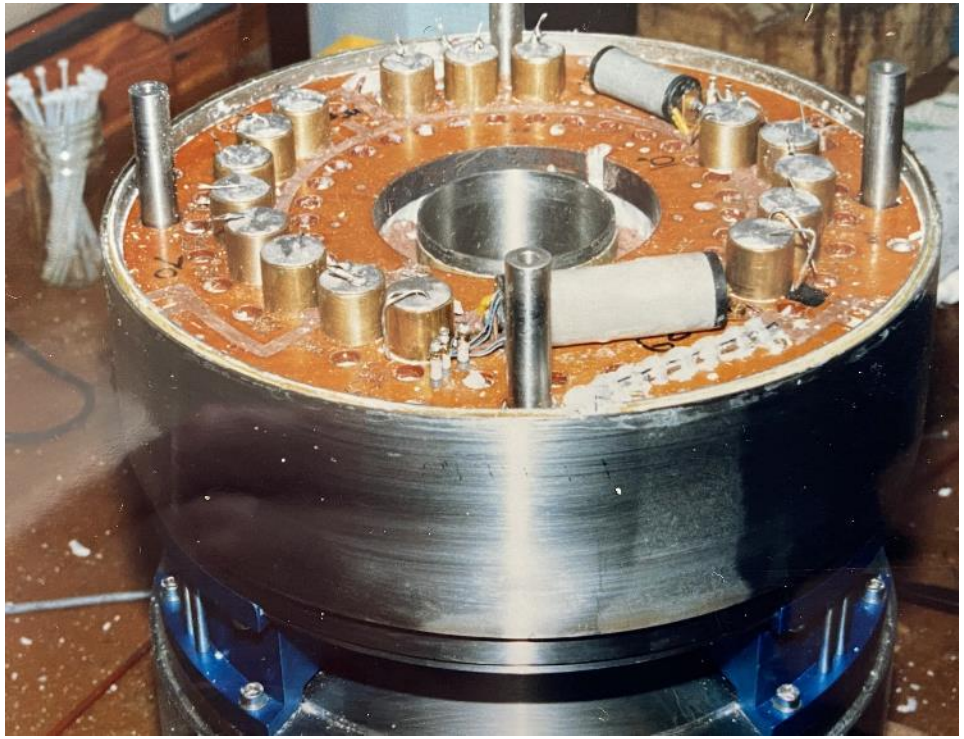

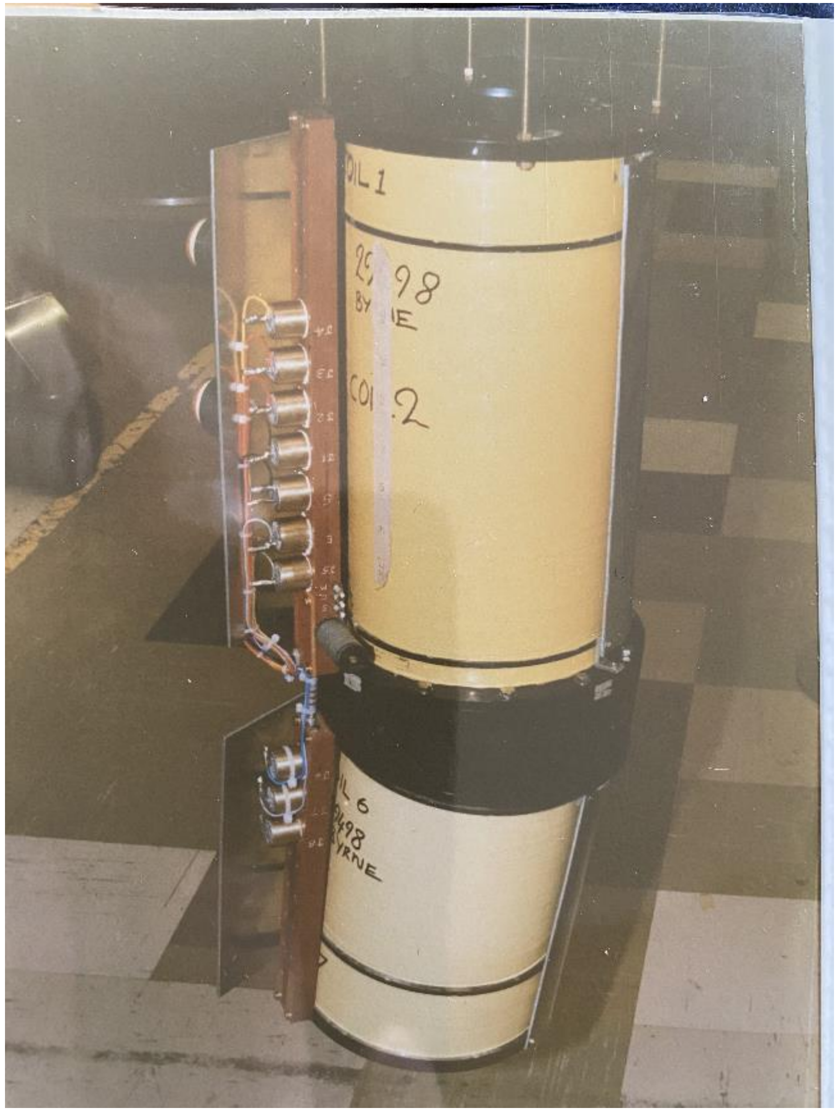

LHC Cable joints

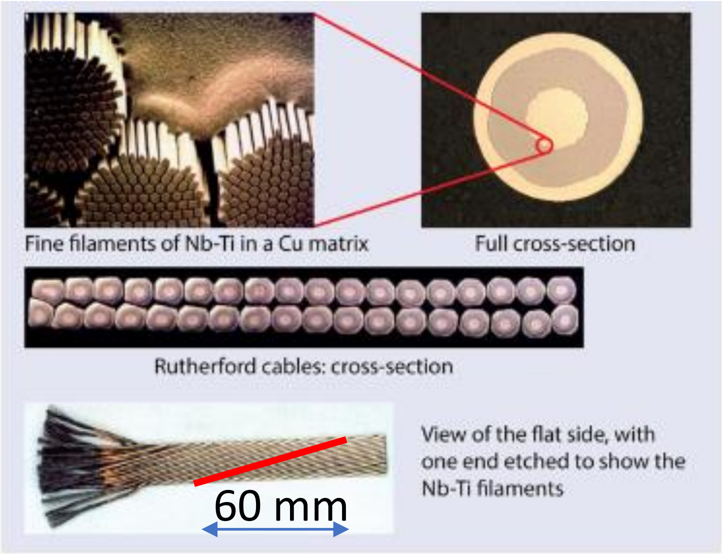

Fig. 2. Structure of the superconducting cable used in the LHC – from Nb-Ti filament to final cable. Credit: CERN

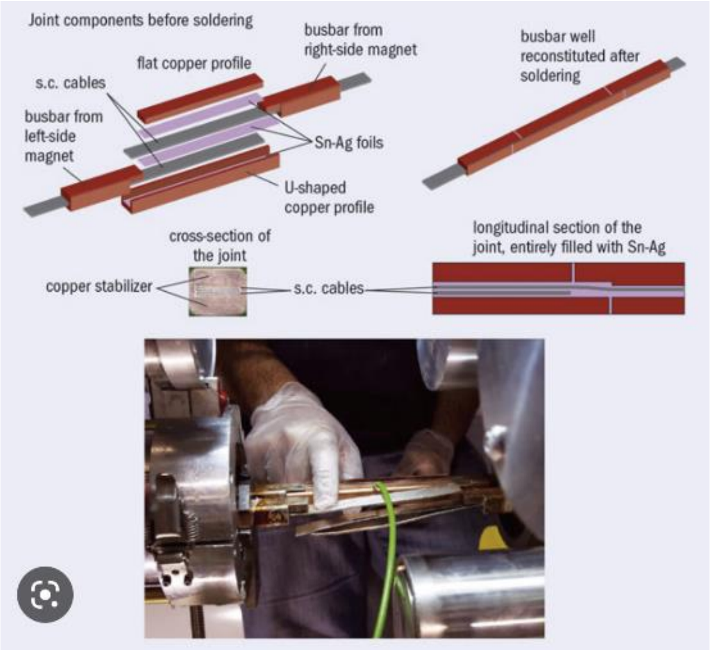

120 mm
Two twist pitches

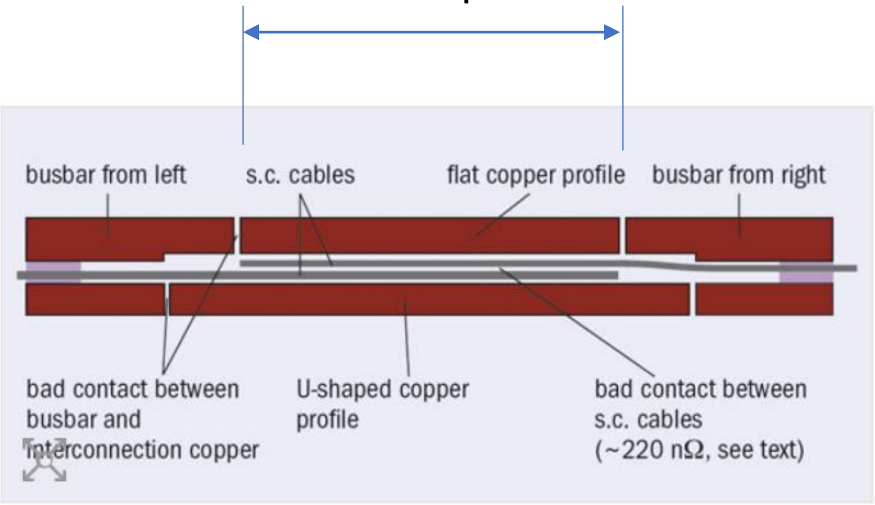

Fig. 3. Schematic of the defective joint assumed to have caused the incident in September 2008.

If you want the 1 nOhm with a std soldered joint, The joint length is the same length weather its 60 A or 10 kA The cable just has more strands.

Joint failure damaged 50 magnet

Target resistance value   1nOhm

Resistance of Splices in the LHC Main Superconducting Magnet Circuits at 1.9 K

Zinour Charifoulline, Mateusz Jakub Bednarek, Reiner Denz, Sandrine Le Naour, Christian Scheuerlein, Andrzej Siemko, Jens Steckert, Jean-Philippe Tock, Arjan Verweij, and Markus Zerlauth

***Abstract*—The electrical interconnections between the LHC main magnets are made of soldered joints (splices) of two superconducting Rutherford cables, stabilized by a copper busbar. In 2009, a number of splices was found not properly stabilized and could have suffered a thermal runaway in case of quench at high current. The LHC was, therefore, operated at reduced energy and all joints were continuously monitored by a newly installed layer of the quench protection system. During the first long shutdown (LS1) in 2013/14, the high-current busbar joints were consolidated to allow us a safe operation of the LHC at its design energy, i.e., 14-TeV center-of-mass. The superconducting magnets and circuits consolidation project has coordinated the consolidation of the 10306 13-kA busbar splices. Since 2015, the LHC is successfully operated at an energy of 13-TeV center-of-mass. This paper will briefly describe the applied analysis method and will present the results and comparisons of the Rutherford-cable splice resistance measurements at 1.9 K before and after LS1, based on an unprecedented amount of information gathered during long-term operation of superconducting high-current joints. A few outliers that are still present after the splice consolidation will also be shortly discussed.**

***Index Terms*—Superconducting cables, superconducting magnets, electrical resistance.**

I. Introduction

THE main superconducting (SC) dipole and quadrupole magnets in each of the eight sectors of the Large Hadron Collider (LHC) [1] are powered in series. Each main dipole circuit (RB) consists of 154 magnets and 156 busbar segments. The quadrupole circuits, focusing and defocusing (RQF and RQD), consist of 47 or 51 magnets and 48 or 52 busbar segments respectively. Both types of busbars are composed of a single 15.1×1.5 mm^2 Nb-Ti Rutherford cable in the center of the copper bar. The only difference is the total busbar cross section, which is $20 \times 16\,mm^2$ for RB circuits and $20 \times 10\,mm^2$ for RQ circuits [2], [3]. The 10306 connections between busbars are soldered by inductive heating using Sn96Ag4 alloy [4]–[6]. During this process, the two superconducting cables are connected (spliced) with an overlap of 120 mm. The expected average splice resistance is about 0.3 nΩ at 1.9 K with a nominal acceptance limit set to 0.6 nΩ for the LHC. The number of splices in a single busbar segment varies from 2 to 6 in RB circuits and from 5 up to 32 in RQ circuits (see Table I). The major part of the busbars by number of splices per segment are the ones with 2 (30%) and 3 (65%) splices in RB circuits, while in RQ circuits they are the segments with 8 (91%) splices. The rest of them are the segments between the first or last magnets in the circuits and the electrical feedboxes located at each end of the 8 sectors of the LHC. In the feedboxes, the current is routed from room temperature to the SC magnets busbars along current leads and SC busbars [13].

TABLE I
BUSBARS IN THE LHC MAIN MAGNET CIRCUITS

Circuit	Busbar cross-section	Num of magnets	Num of busbar segments	Num of splices per segment
RB	$20 \times 16\,mm^2$	1232	1248	2–6
RQD/F	$20 \times 10\,mm^2$	392	800	5–32/21 [a]

RB corresponds to the main dipole circuit, RQD/F to the main quadrupole circuits (defocusing and focusing).
[a] The 32 splices busbar segments have been shortened during LS1.

A. nQPS: Busbar Protection and Monitoring

Since 2009, every busbar segment in the LHC main magnet circuits (RB and RQ) is monitored by the so-called DQQBS boards, representing one of the major components of a newly installed layer of the Quench Protection System (nQPS) [7], [8]. Protection boards provide an early detection and warning in case superconducting busbars or splices develop excessive resistances. Each DQQBS board has two analogue channels, U_BUS and U_MAG, where U_BUS is measuring the busbar voltage, while U_MAG is measuring the adjacent magnet voltage. The magnet signals are hereby used for the compensation of the inductive part of busbar voltages during current ramps. In addition to the main protection functionality, the nQPS provides continuous data for long-term storage within the LHC logging database, providing the basis of the measured voltages and the circuit current values used for splice resistance calculations. The main technical characteristics of nQPS boards are summarized in Table II. More detailed information about the nQPS installation and the functionalities of its protection boards can be found in a series of publications already presented in different conferences [7], [8], [10].

Manuscript received August 27, 2017; accepted December 12, 2017. Date of publication December 18, 2017; date of current version January 19, 2018. *(Corresponding author: Zinour Charifoulline.)*

The authors are with the CERN, Geneva 1211, Switzerland (e-mail: zinour.charifoulline@cern.ch).

Color versions of one or more of the figures in this paper are available online at http://ieeexplore.ieee.org.
Digital Object Identifier 10.1109/TASC.2017.2784355

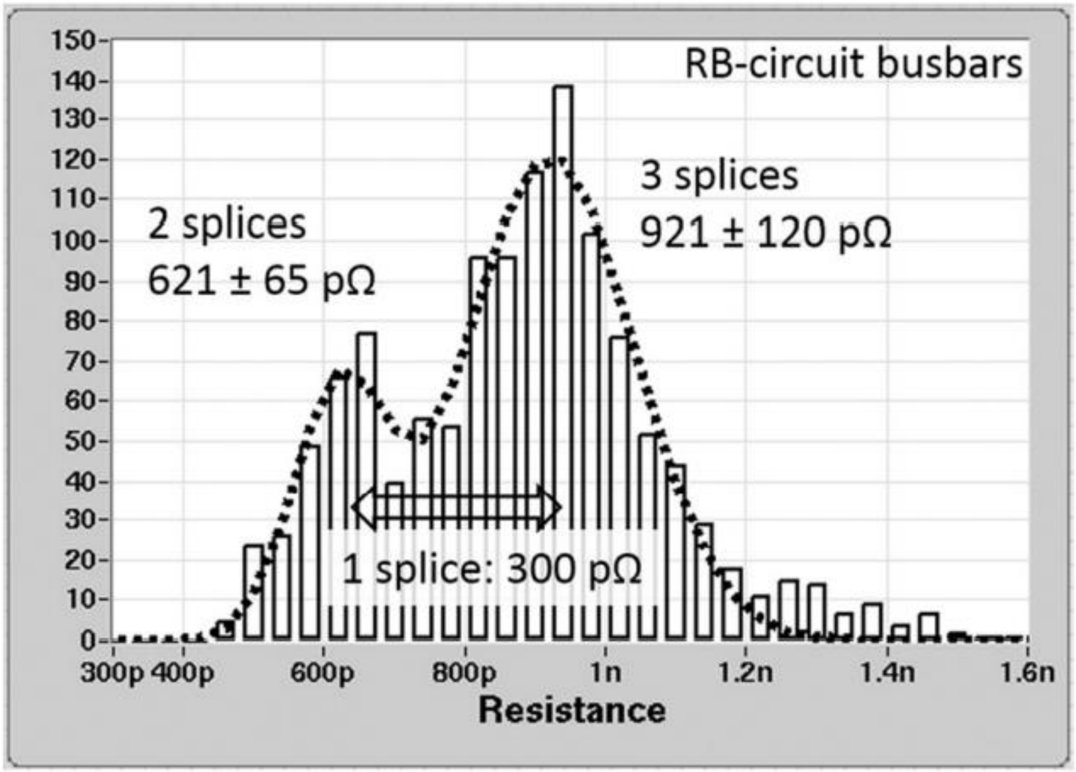

Fig. 2. Gaussian fit of the RB-circuit busbar segment resistances where 368 segments have two and 816 segments have three splices.

Fast ramping joint resistances

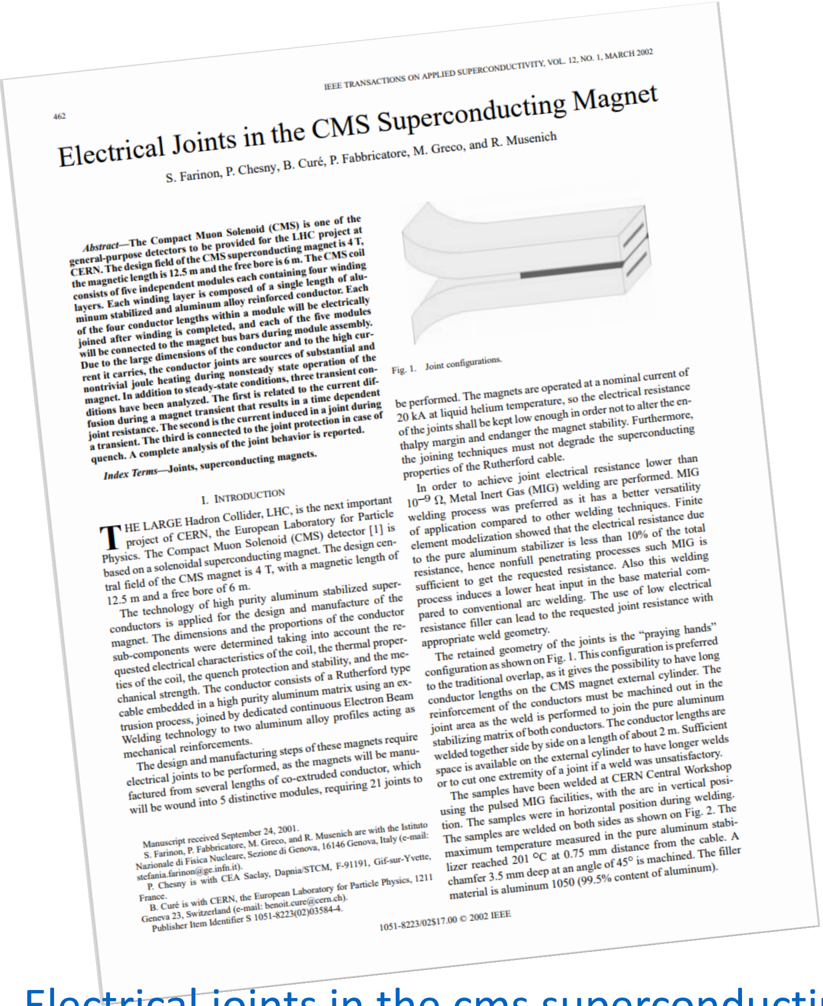

IEEE TRANSACTIONS ON APPLIED SUPERCONDUCTIVITY, VOL. 12, NO. 1, MARCH 2002

462

Electrical Joints in the CMS Superconducting Magnet

S. Farinon, P. Chesny, B. Curé, P. Fabbricatore, M. Greco, and R. Musenich

Fig. 1. Joint configurations.

1051-8223/02$17.00 © 2002 IEEE

IV. Discussion

As obtained by the solution of the diffusion equation and confirmed by the measurement results, the voltage drop and, in turn, the joint resistance show a strong time dependent behavior. With respect to the steady state value, the voltage drop reaches very high values (more than twice with current rates up to 20 A/s), then it decades with a time constant depending on the applied field. In terms of dissipated power that means a peak value, at $B = 0$ T, of 45 mW with respect to a steady state value of 39 mW.

The fit with the analytical expression is in good agreement with the measurements, excluding the low current regions where oscillations of the power supply occur (the reported current vs. time curves are the imposed ones).

The decay time and the steady state resistance values are respectively 1700 s and 0.39 nΩ at $B = 0$ T and $B = 1$ T, and 1460 s and 0.454 nΩ at $B = 2$ T. As expected, the decay time is perfectly proportional to the reverse of the steady state resistance.

A question arises about the consequences on the magnet operation. Considering a steady state joint resistance of 0.39 nΩ, and the 5 h charging time foreseen for the CMS magnet (up to 20 000 A), the voltage peak value is only 3% higher than the steady state one. Lower values of the joint resistance lead to higher voltage ratios, but the effect on the magnet behavior is negligible.

Joint inductance can give higher voltages with ramping of the current !

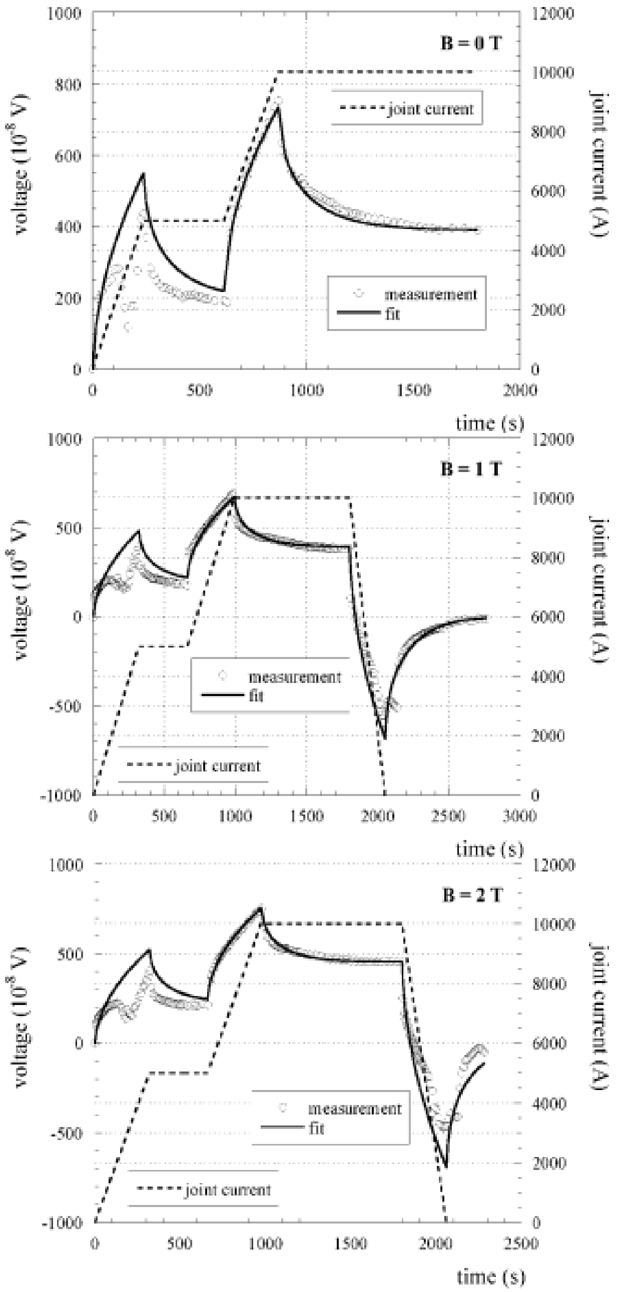

Fig. 5. Measured voltage drop across the joint at the applied fields $B = 0$ T, $B = 1$ T, and $B = 2$ T, compared with the results of the fit with the analytical expression. The joint current is shown as well.

[Electrical joints in the cms superconducting magnet - Applied Superconductivity, IEEE Transactions on (infn.it)]

Joint box (80 joints)

You
added an **update**

Dec 13, 2022

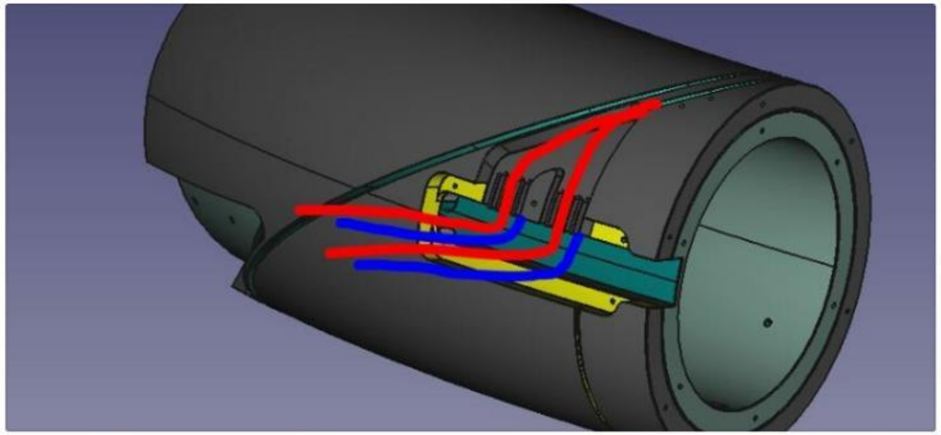

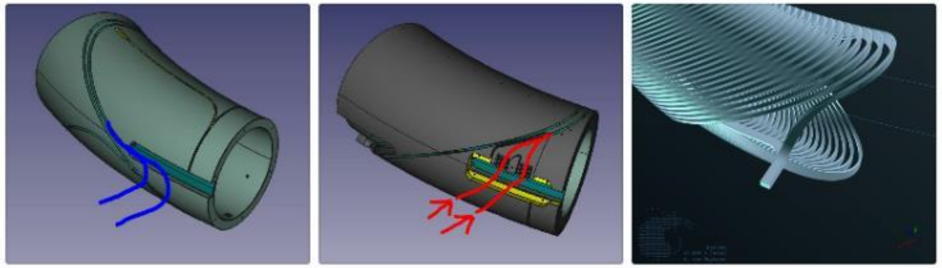

Improving the magnetic model

the magnetic model did not have the leads that come from the coil to the joint box. By adding the leads we can improve the model. The three imagines show the nominate path that the cables take. The field is cancelled where the strands run next to each other. as they separate the field starts to be generated.

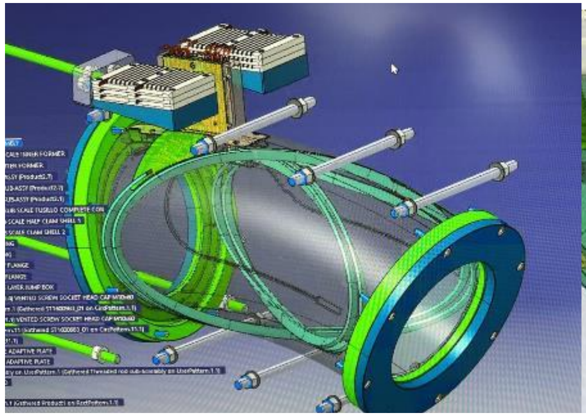

Sub scale coil will test this plan

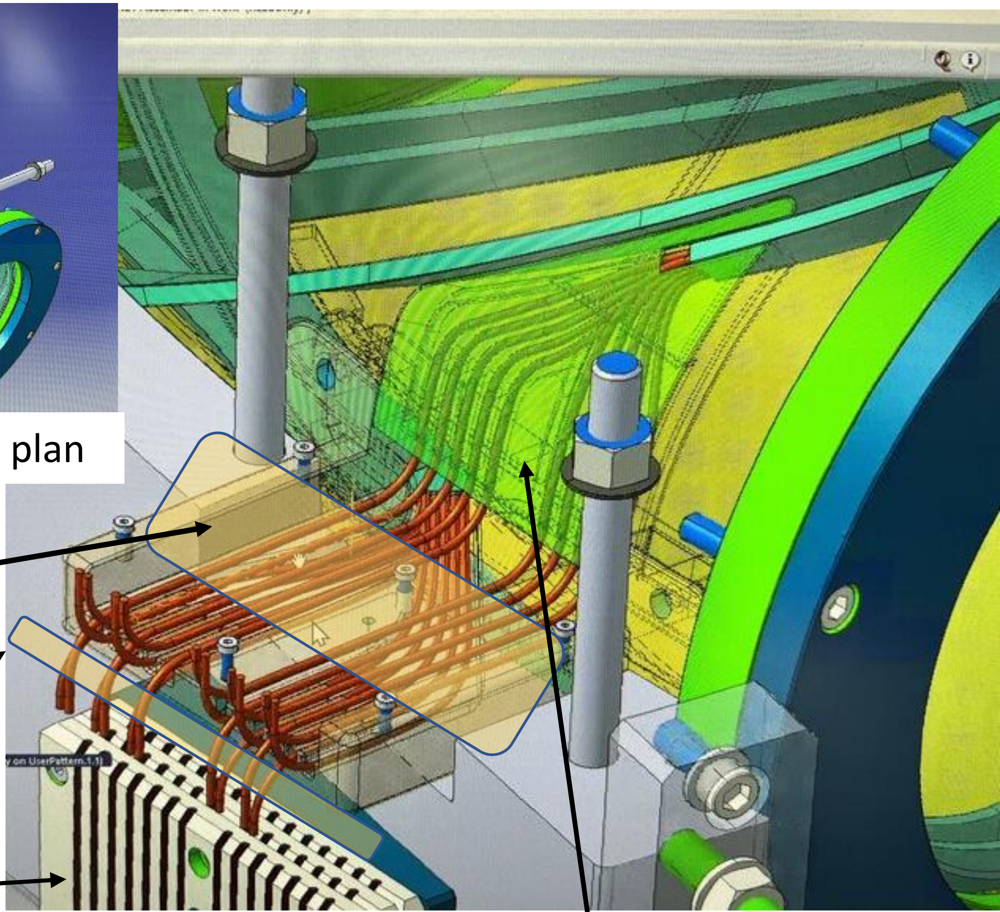

Sealing zone 2

V tap box zone 3
(not yet in the design)

Joints box zone 4

Separating zone 1

4 zone joint box

- The 7 strand ropes exit the channel and are separated.
- There is a sealing zone for the impregnation
- Voltage tap box (not yet in the design)
- Then the individual wires are supported and guided to the 150 mm long joint that is in liquid !

Joint box Development

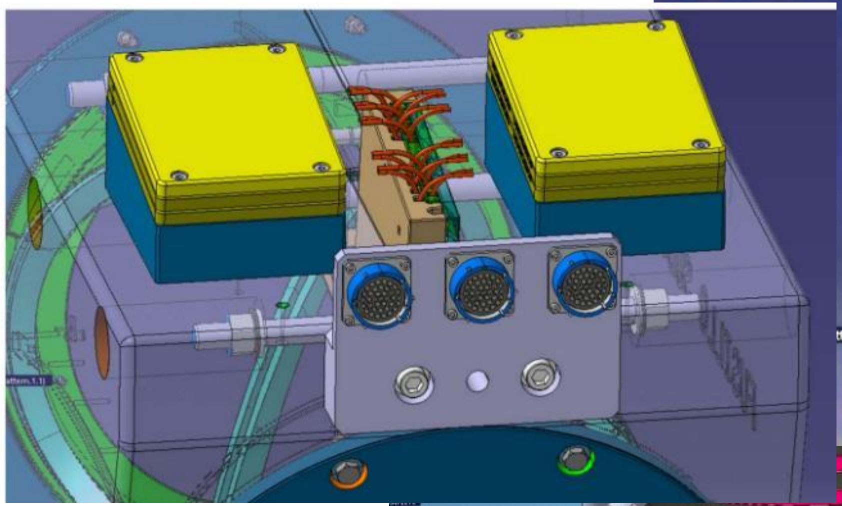

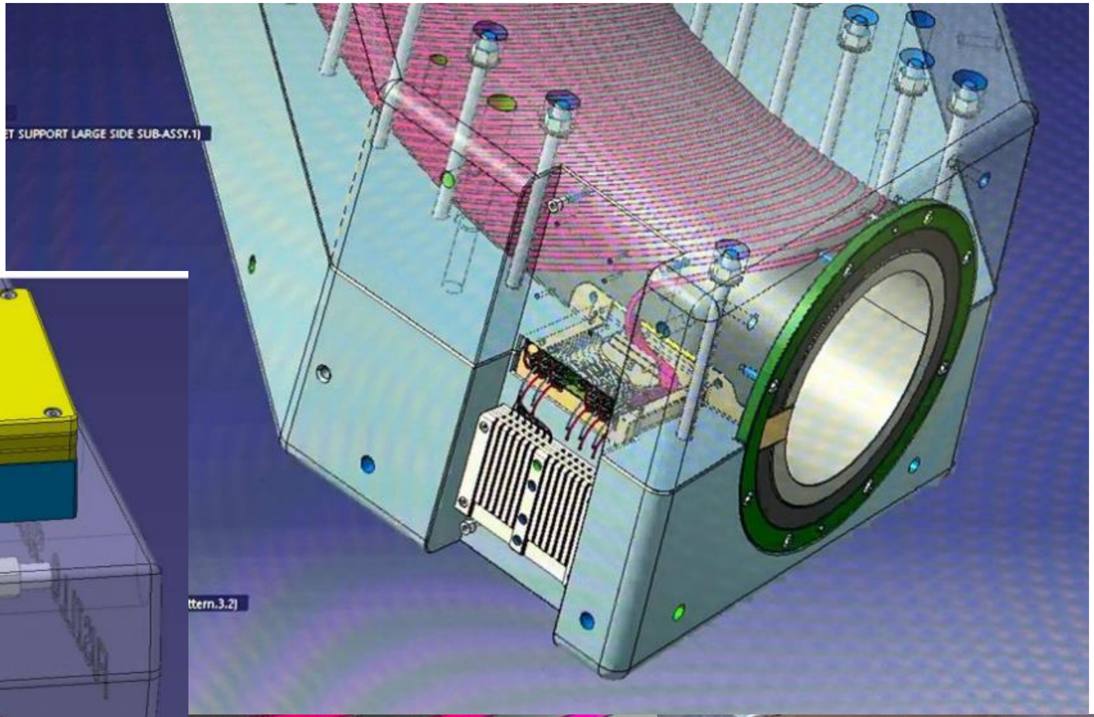

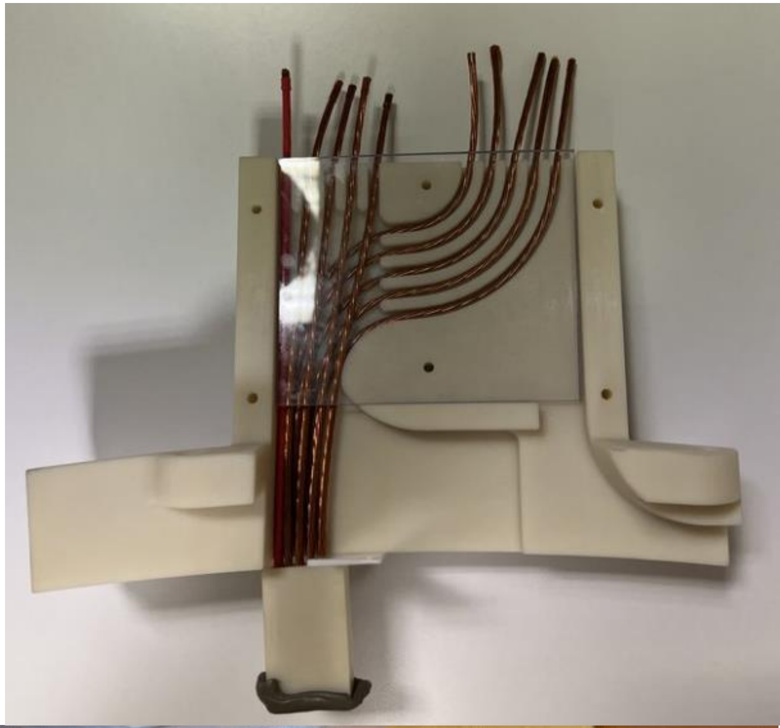

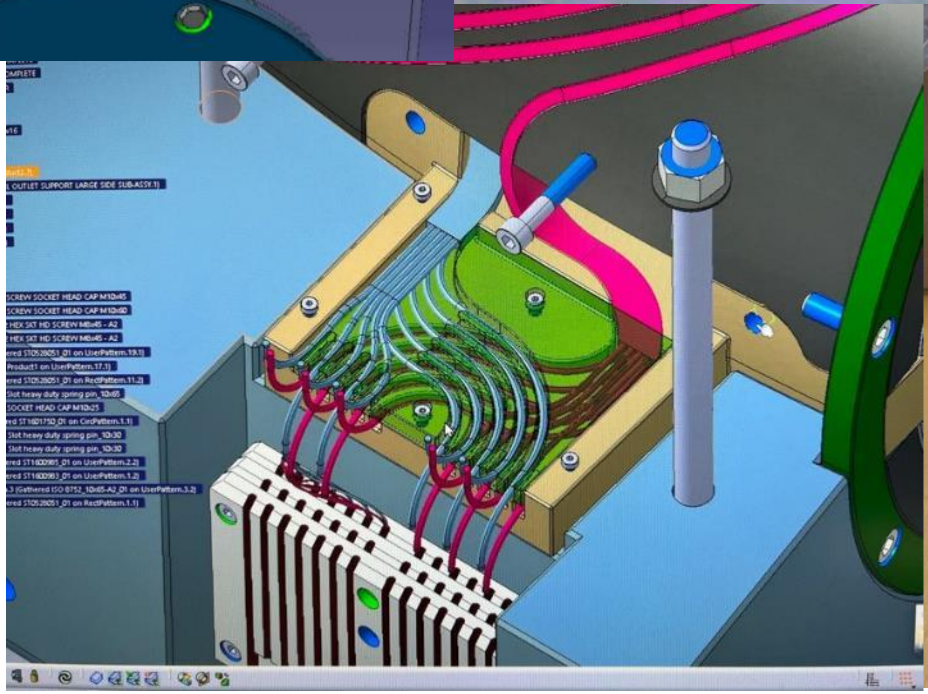

Joint subjects not covered in this talk

- Friction welded mono-filament joints
- Nb_3Sn Joints (resistive and persistent)
- Conduction cooled joints with cryocoolers
- The zoo of HTS joint designs a big subject.

Notes on Test Coil Winding

Winding tests

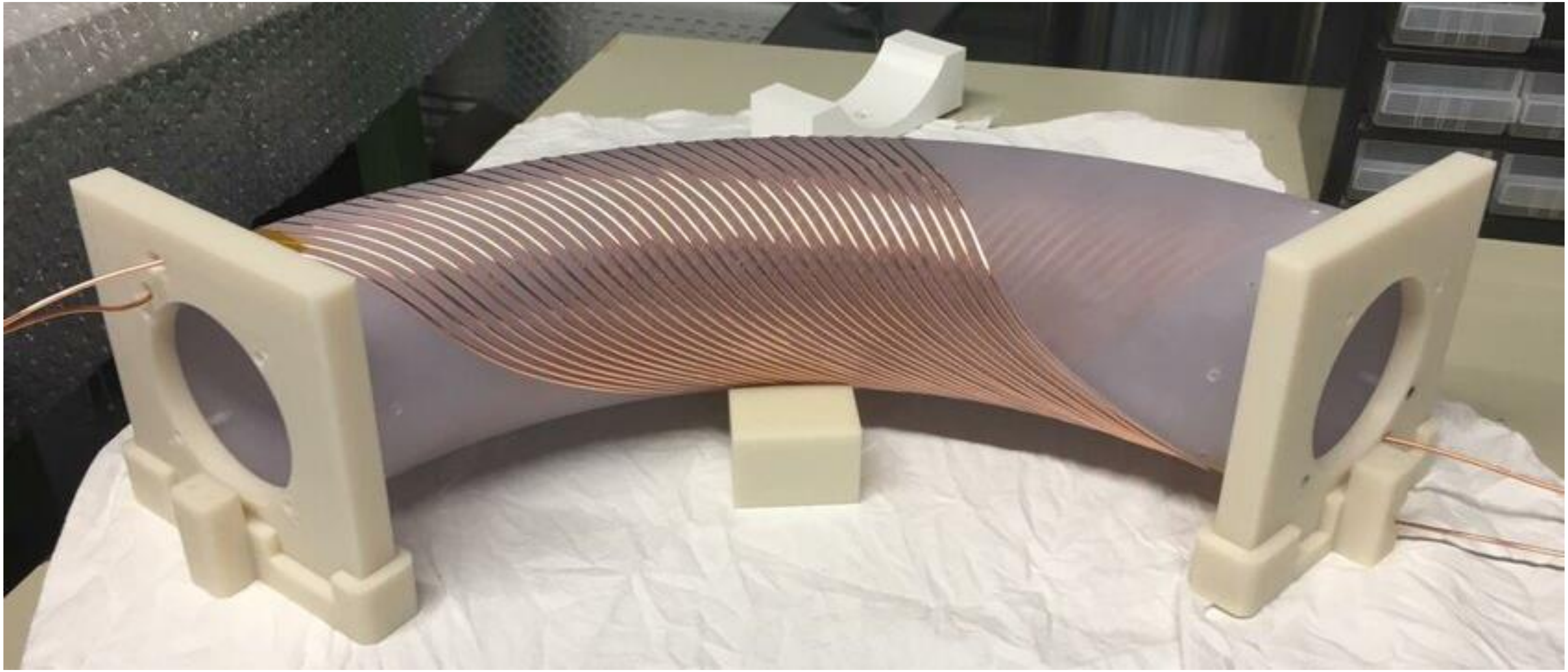

Winding tools for subscale

Pre guide and hand tool

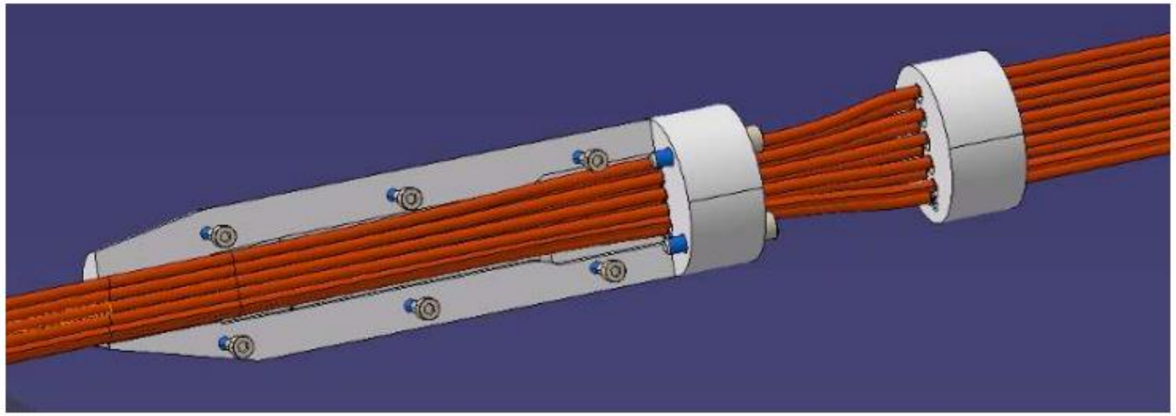

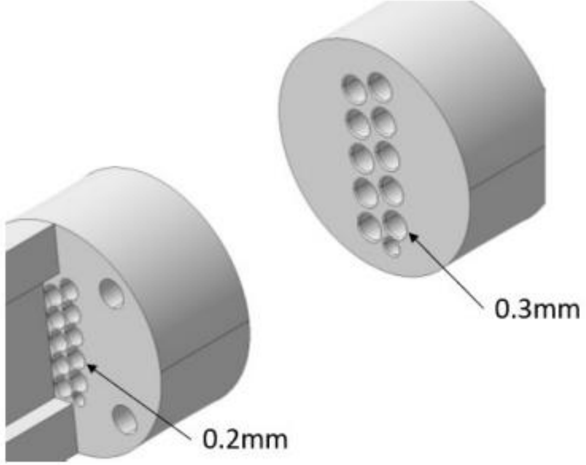

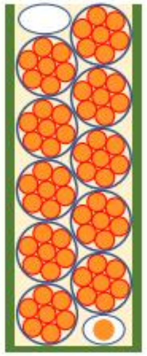

Pre guide 1
Diameter : 4.5 mm

Pre guide 2
Diameter : 3.4 mm

Guide
Diameter : 3.2 mm
Exact position

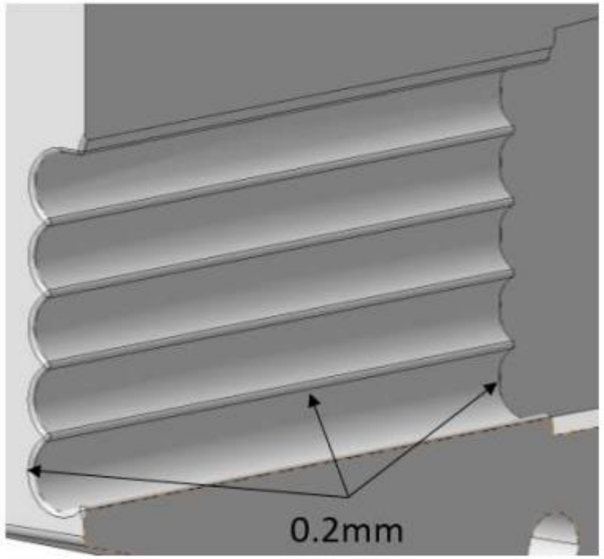

Winding instability

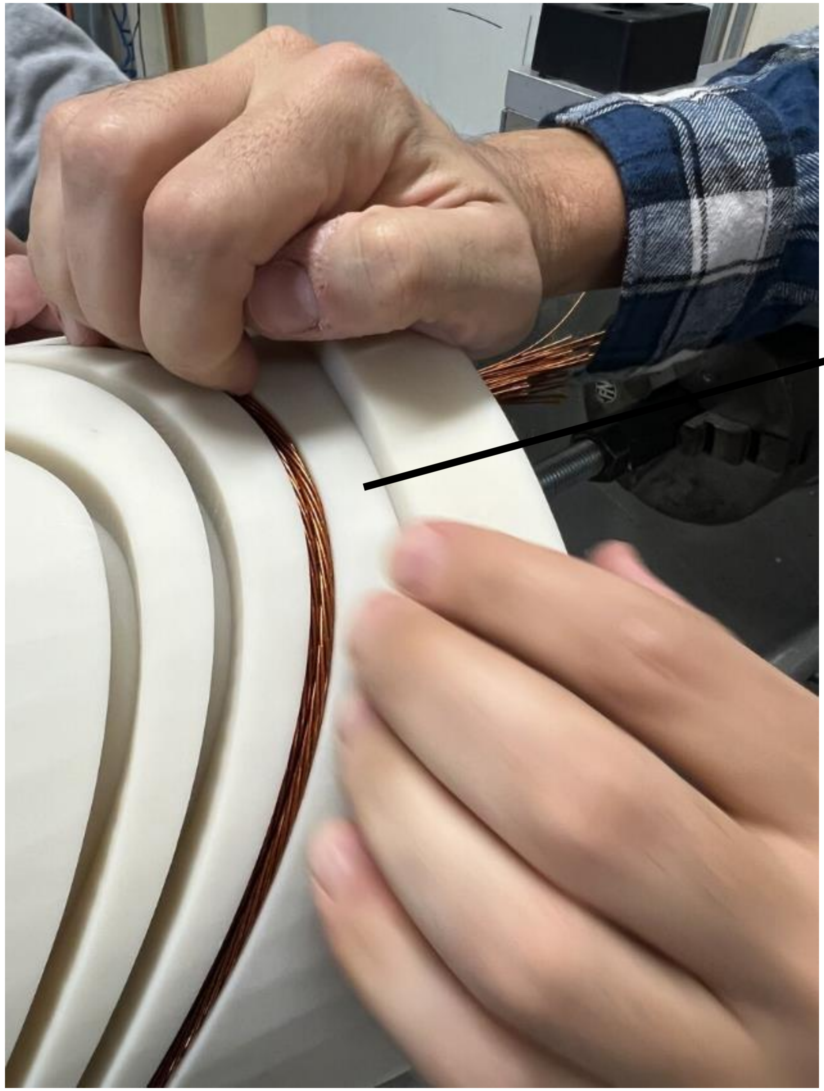

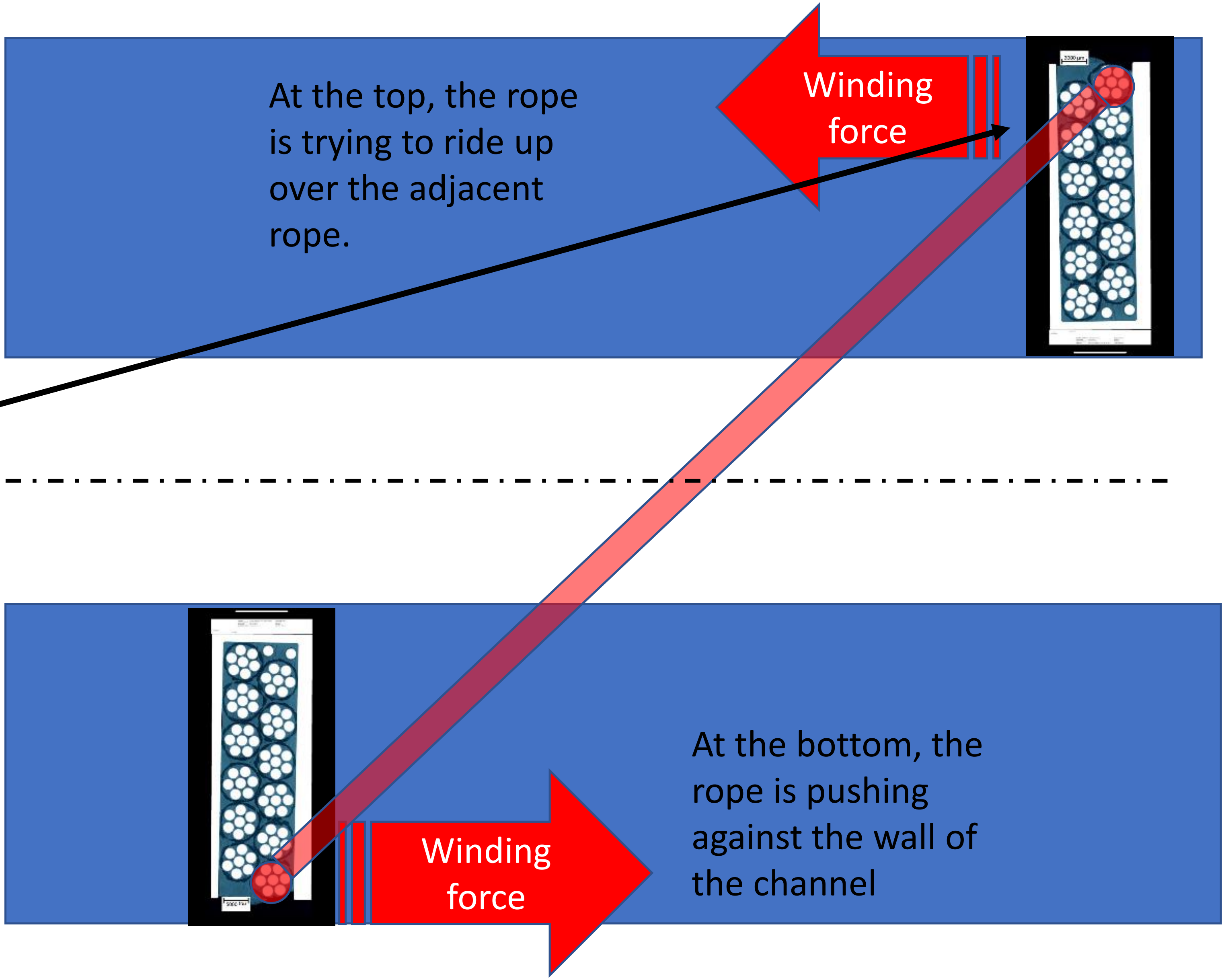

You
added an **update**

Oct 20, 2022

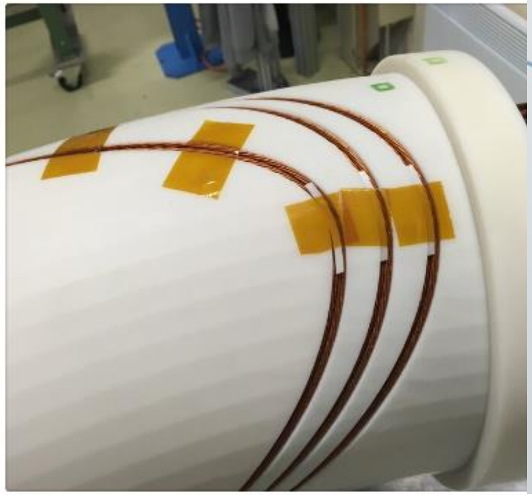

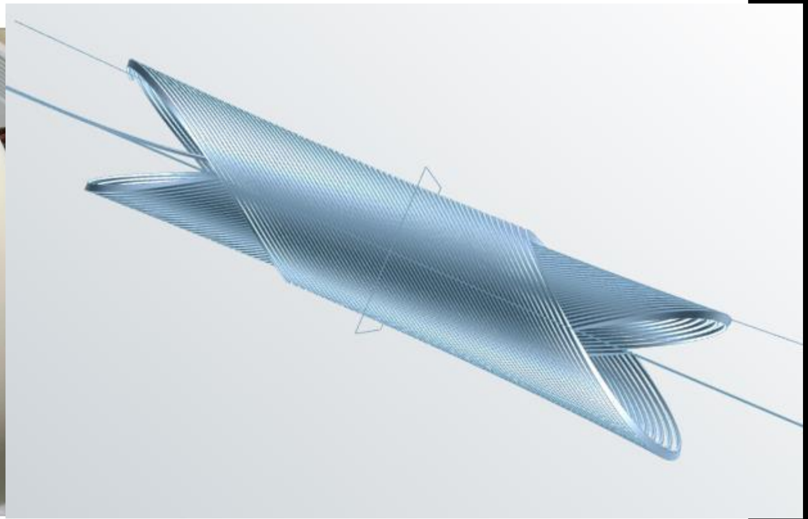

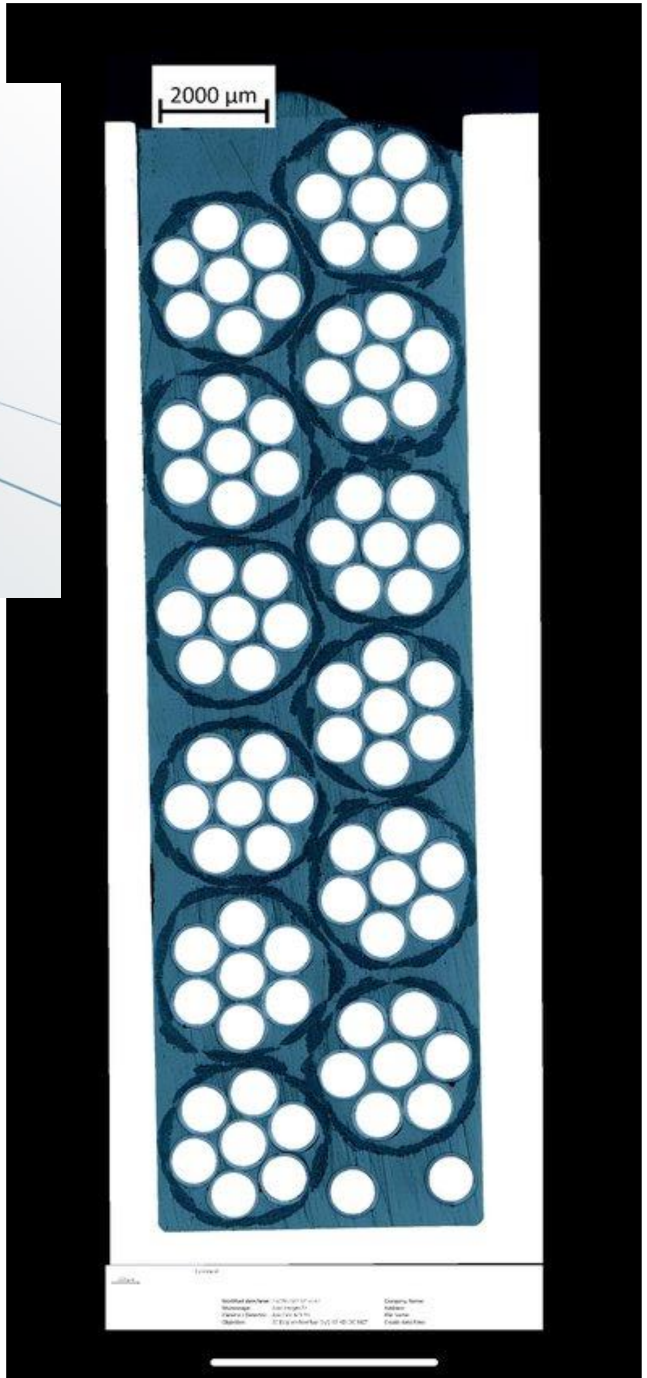

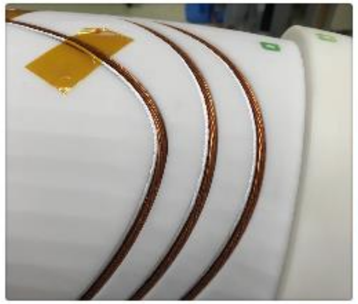

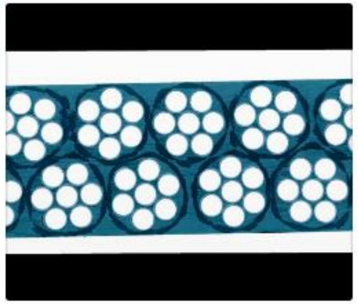

More on coil winding

3 D printed spacers helped to keep the top rope turn in the good place during winding. It was soon realized that we need this support over the full turn. So the printed spacer was replaced with a fiber rope that we had. not the perfect size but did the job. the same problem will exist at the bottom the channel. We want to place a set of insulated wires at the bottom in the space next to the bottom rope. But again it wants to move over from top to bottom as we wind the coil. Yet to be solved.

3D printed inserts

At first, we put spacers top to hold the top part of the cable in place

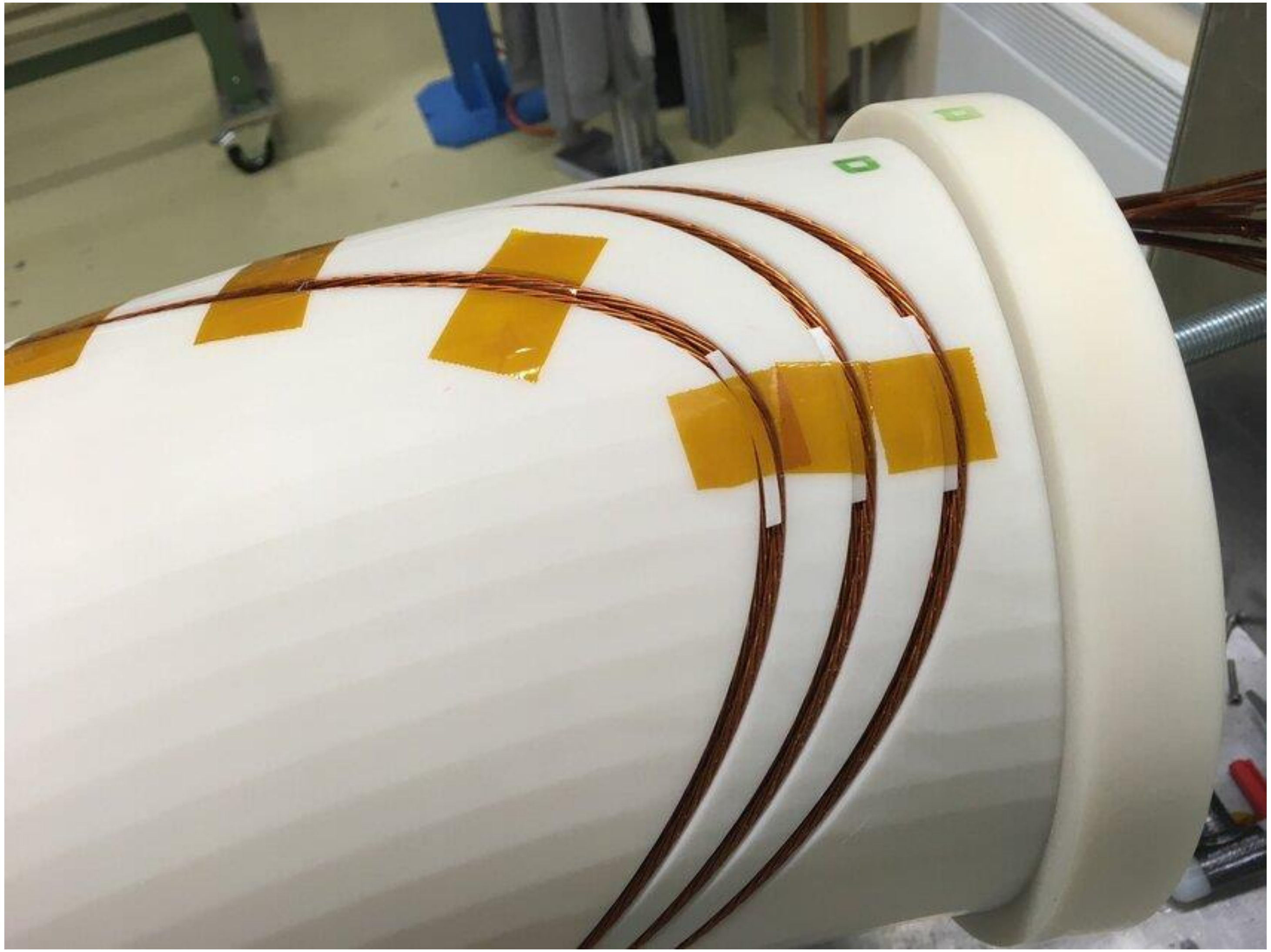

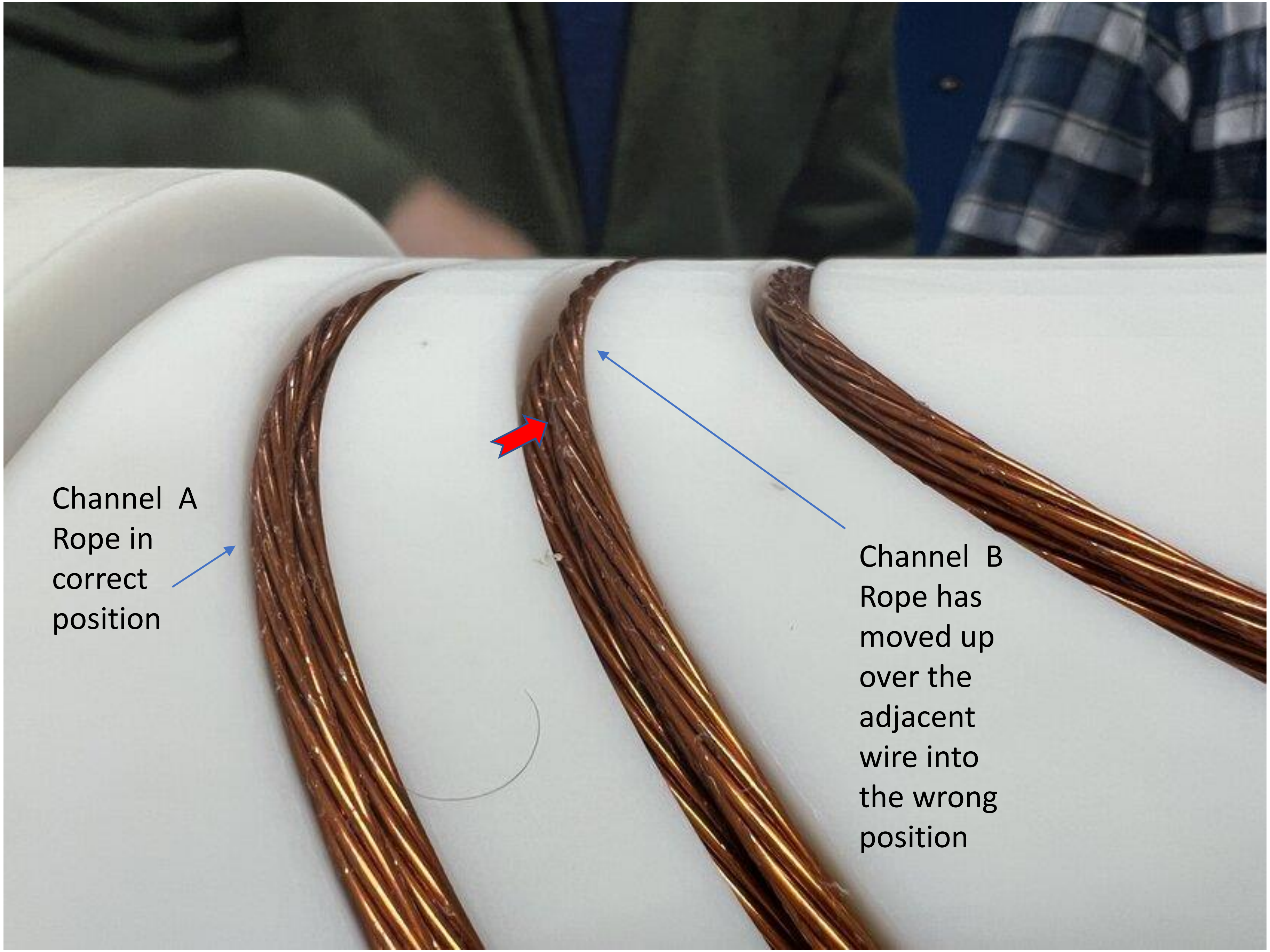
Channel A
Rope in
correct
position
Channel B
Rope has
moved up
over the
adjacent
wire into
the wrong
position

Additional glass rope

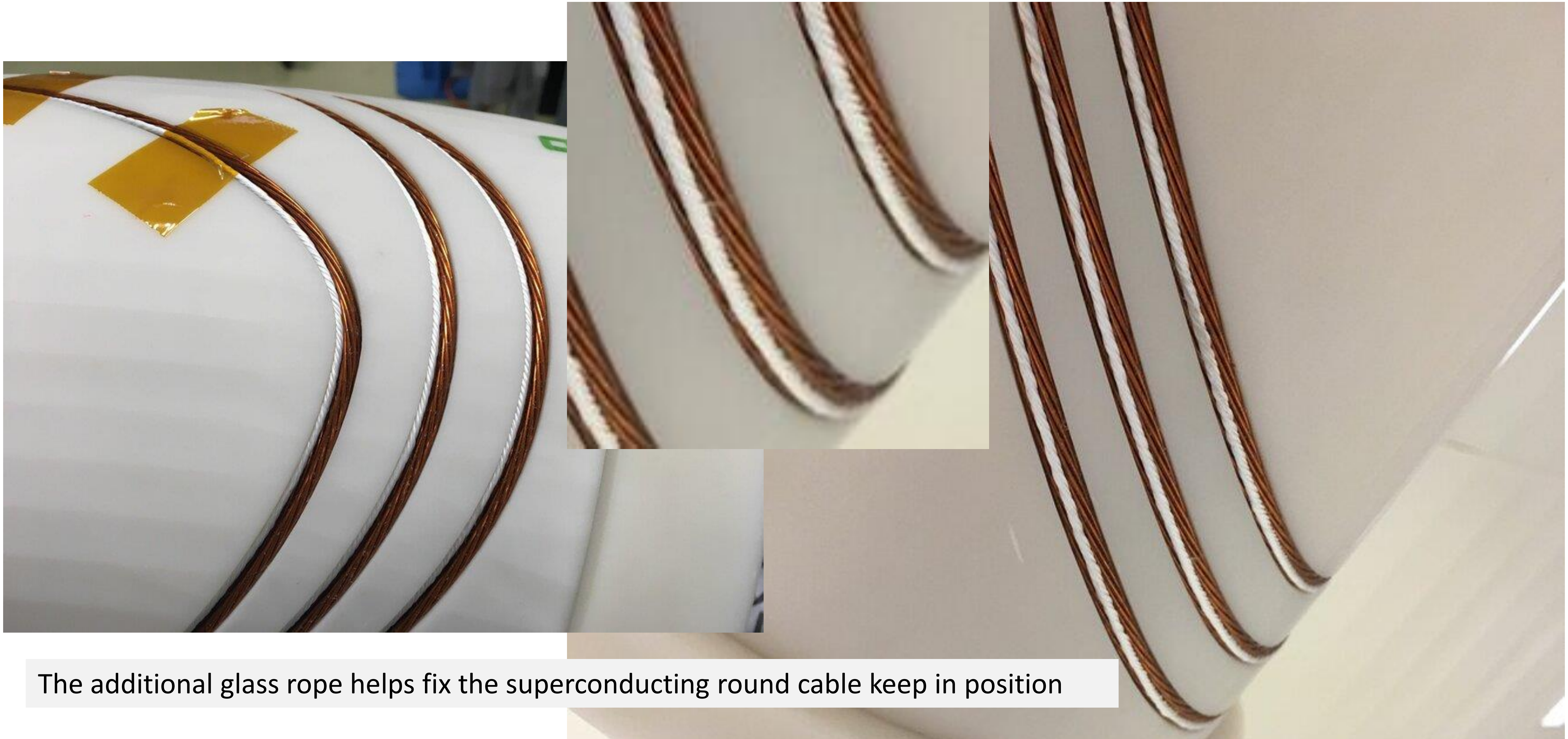

The additional glass rope helps fix the superconducting round cable keep in position

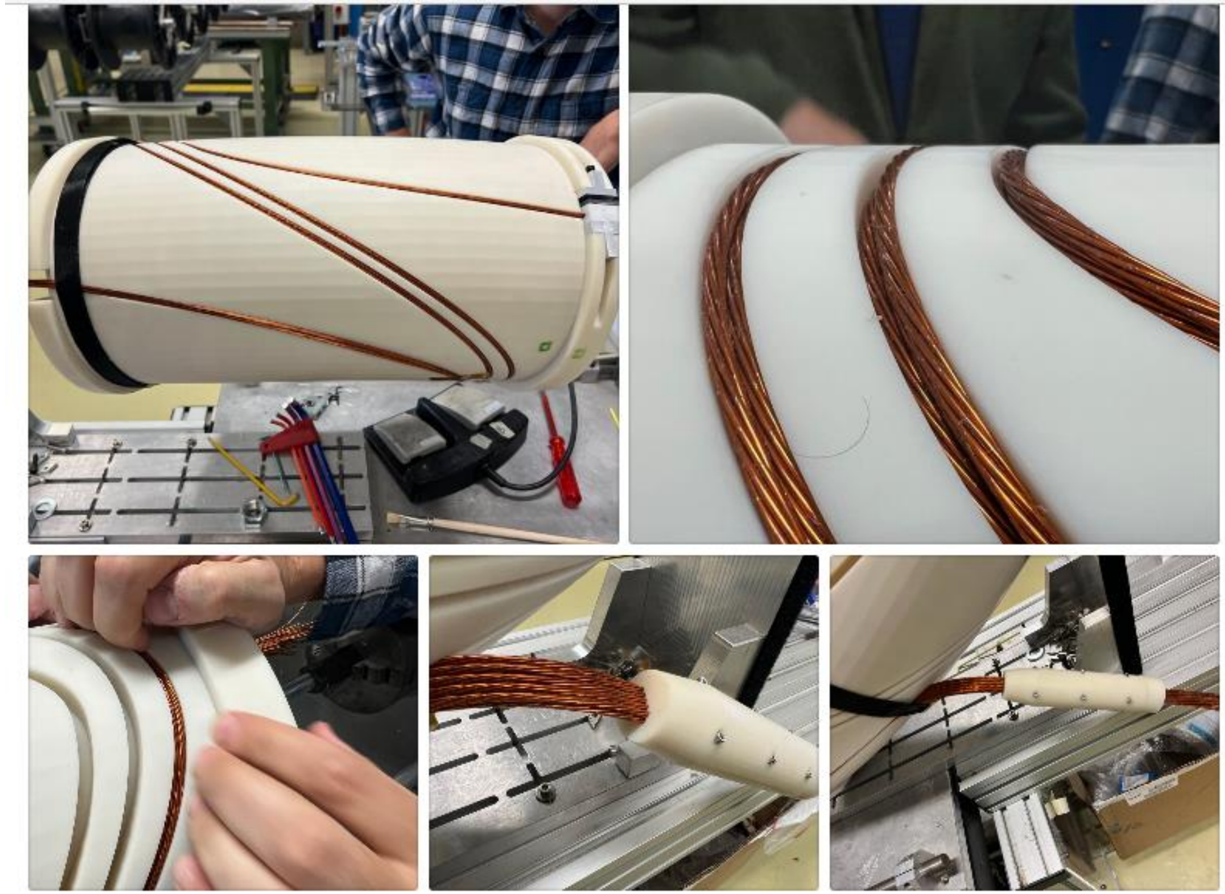

Winding tests highlight some important points

Today we have been test winding the 3D printed test former with the log-stacking layout. We will need to add some small half moon spacers at one end of the coil to hold the outer most rope in the outer location. magnetic force is in the direction to push the rope towards the direction of the channel wall, that is closest to the rope. But during winding that last rope can fall into the wrong place. We imagine the same problem at te bottom of the channel. Very productive test !

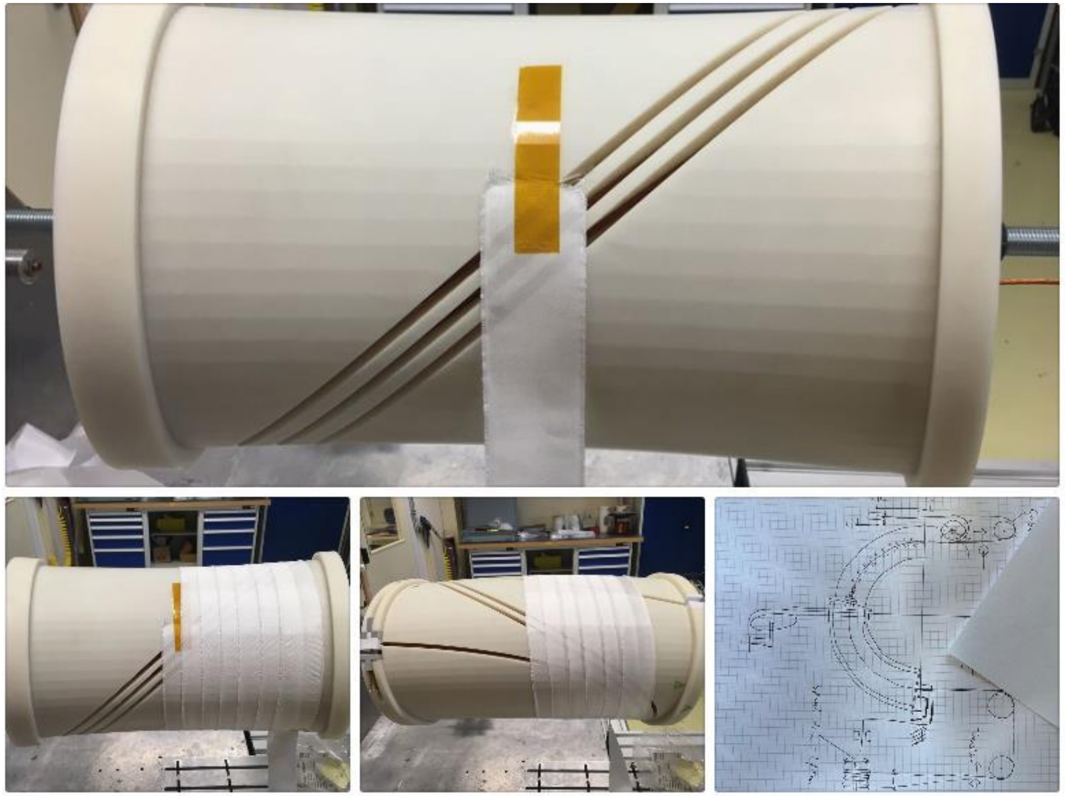

Fusillo Inter-layer insulation glass and kapton assembly

We are testing how to apply the glass tape and kapton insulation to the curved formers. this is the start of a development needed to be able to apply the insulation and glass tape in a uniform accurate way. The wide tape has a 49% overlap on the inner edge. So just two layers. then reduces at the outer radius to have about 37.5% overlap. This leaves about a 5 mm opening From the half overlapped position that is on the inner edge. We start to look at tooling ideas that could wrap the tape. The sketch shows the former rotating. With a 100 deg curved track. Each rotation the former is moved along the curved arm by one half pitch of the tape width. Pulled by a cord that winds onto a spool. Just one of the ideas.

Sub-scale winding test

Note the cable clamp system

You
added an **update**

Aug 3, 2022

Winding test on sub turn former

The 3D printed glass filled Nylon former is being used to asses coils winding, the tooling, effect of wall thickness exaggerated deflection. Will the clamping system damage the rope cable insulation. The glass sleeve although not needed for insulation it will give protection during winding and help with impregnation. However if the magnetic field required to be increased this could be an option be removed to increase Ic of the coil pack. You can also see the short channel stacking test. This will be impregnated, see a thermal cycle , cut , polished, and inspected.

Dani's, you tube films & Mike's idea's

We have been developing an external tube to hole the wires in the channel.

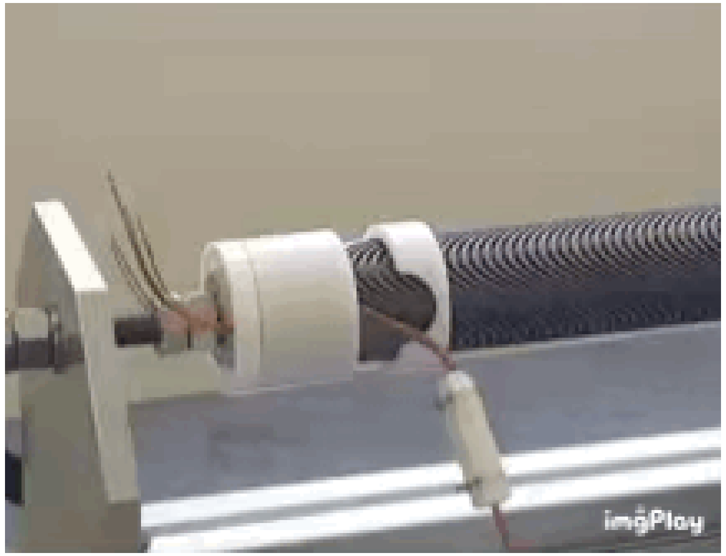

Mike's original idea small quad

Coil winding Dani's Sushi CCT

https://www.youtube.com/playlist?list=PLeC-OFQnTJU_-4SBEik2P-025CHFe9ZzN
https://www.youtube.com/watch?v=1BVQtau7L5w
https://www.youtube.com/watch?v=7x09XcfOCsE

https://youtu.be/jziguNhHCg8

Coil winding machine is still under discussion

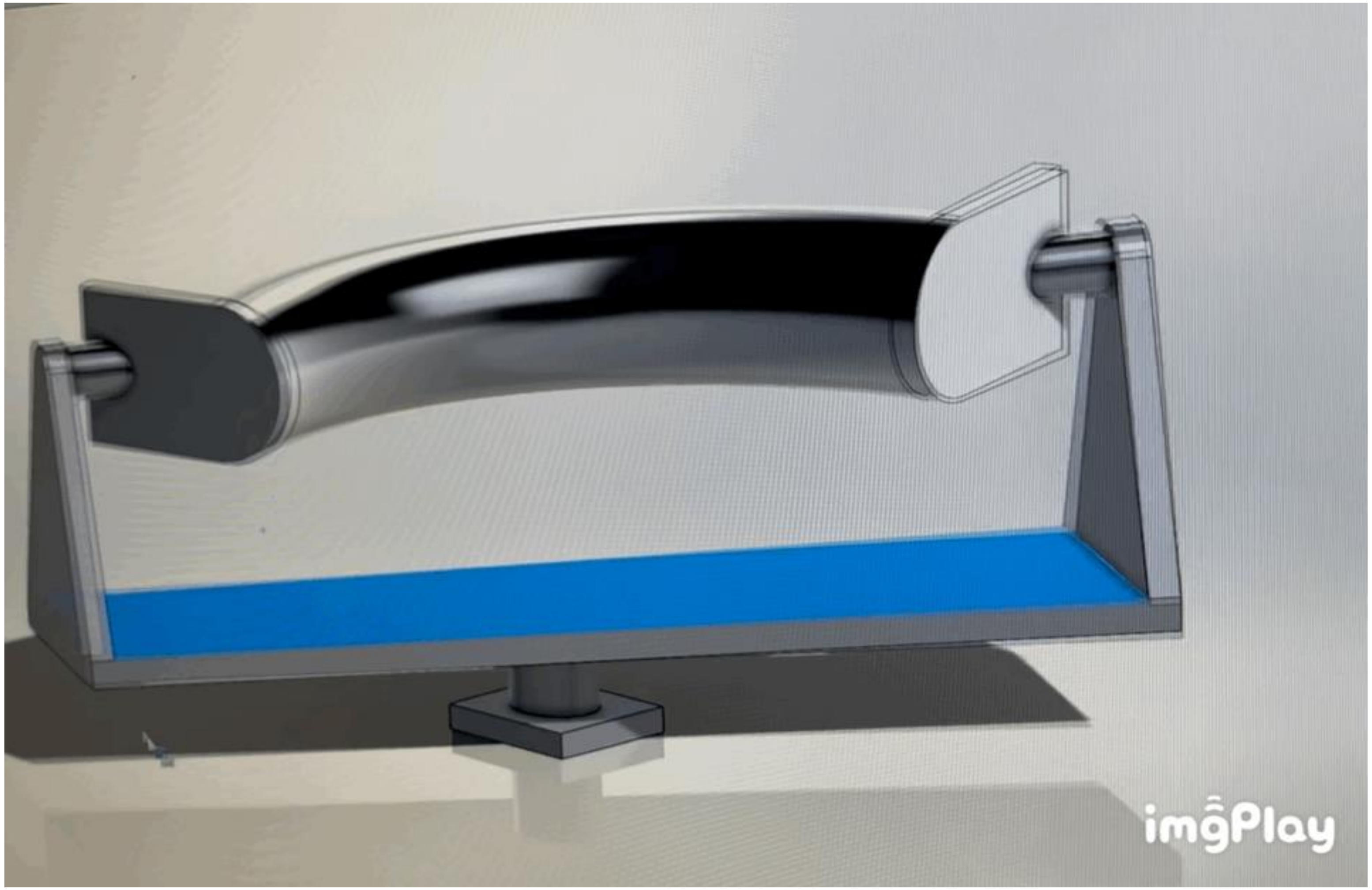

Thanks to Oliver for the animation

The End